Egyptian Journal of Aquatic Biology & Fisheries
Zoology Department, Faculty of Science,
Ain Shams University, Cairo, Egypt.
ISSN 1110 – 6131
Vol. 26(5): 1241 – 1271 (2022)
www.ejabf.journals.ekb.eg

Susceptibility of El-Alamein coast to contamination and future prediction of erosion using geostatistical analyses

Ahmed El-Zeiny[1], Hanaa Hammad[1*], Mohamed Abu El-Hassan[2], Moataz Khalifa[2]

1. Environmental Studies Department, National Authority for Remote Sensing and Space Sciences (NARSS), Egypt
2. Geology Department, Faculty of Sciences, Menofia University, Egypt

[*]**Corresponding Author: geo.hanaa.adel@gmail.com**

ARTICLE INFO

Article History:
Received: June 27, 2022
Accepted: Sep. 27, 2022
Online: Oct. 28, 2022

Keywords:
Water pollution,
Sediment pollution,
El-Alamein coast,
Remote Sensing,
Geostatistical analyses.

ABSTRACT

Investigating heavy metal levels and the associated contamination of water and sediments are crucial issues to ensure the sustainability of the ecosystem in the future, especially in marine zones. This study is aiming to assess water/ sediment quality and contamination indices of El-Alamein coast, in addition to predicting the shoreline in 2030 and the erosion/ accretion rates from 2020 to 2030 using spatial and statistical techniques. To fulfill this aim, 25 water samples and 21 sediment samples were collected from the Mediterranean coast and the connected artificial ponds during the period from November 13th to 14th, 2020. Physico-chemical parameters, nutrients, and four heavy metals were investigated (Cd, Pb, Ni, Fe) since the geostatistical analyses tool (IDW technique) in ArcGIS 10.5 software was used to present water and sediment analyses/ contamination indices in spatial distribution maps. Moreover, the Digital Shoreline Analysis System (DSAS) tool was used to predict the 2030 shoreline, erosion, and accretion rates. Results indicated that the middle region of the shoreline is the most affected part by contamination, especially Cd, ranging from 0.06 mg/l to 0.17 mg/l and from 1.68 mg/kg to 3.57 mg/kg in water and sediment, respectively. The metals contamination indices in sediment highlighted that the Cd Contamination Factor was very high, the Cd Ecological risk was high to very high, the Cd and Pb Enrichment Factors were extremely high, and the Cd Geo-accumulation index was moderate to heavy. However, the overall indices assessment indicated the following: the risk index revealed a low level of risk, the pollution load index showed no pollution, and the degree of contamination was mostly moderate. There will be a shoreline retreat in 2030 showing elevated accretion (1.793 km^2) than erosion (0.361 km^2). It's recommended to monitor the coastal changes and water/ sediment quality regularly to detect any changes that might occur to prevent the probable effect on El-Alamein marine ecosystem.

INTRODUCTION

Everything that rivers carry away eventually ends up in the sea. As a result, sewage, rubbish, agricultural waste, and pesticides pollute the environment. The discharge of oils and petroleum products, as well as the dumping of radioactive waste into the sea, add more levels of heavy metals to the marine environment. Pollutants are produced where people live and work, and hence find their way into marine regions nearby their sources. Turbulence and ocean currents may disseminate the contaminant, or other physico-chemical processes such as adsorption, precipitation, and accumulation may concentrate it in food chain components or bottom sediment **(El-Matary, 2006)**.

Monitoring heavy metal levels and analyzing their contamination levels in sediments, on the other hand, are critical and necessary challenges to ensure the ecosystem's long-term viability. Heavy metals analyses in sediments are also fundamental for determining their effects on water and aquatic life. Due to their probable carcinogenic impact, extended persistence, and bioaccumulation qualities, heavy metals have recently received more attention in water research **(Censi *et al*., 2006)**.

Heavy metals naturally occur in the crust of earth and are discharged into the environment through a variety of human activities. Sewage and home cleansers, petroleum wastes, air deposition, industrial effluents, surface runoff, and agricultural discharge water can all contribute to their presence in aquatic habitats **(Mortatti and Probst, 2010)**.

Due to the rising human populations and associated environmental threats, marine water monitoring and assessment have become an integral aspect of marine water management **(El-Zeiny *et al*., 2019)**. Monitoring techniques range from simple testing to expert analyses of the ecosystems' physicochemical and biological features **(Jones and Lee, 1986; Cooke *et al*., 1993; Zeng and Rasmussen, 2005)**. Temporal changes may be readily tracked, and harmful impacts can be reduced by monitoring the physicochemical and microbiological features of the aquatic ecosystem **(Bhateria and Jain, 2016)**. Monitoring spatial-temporal changes of coastal environments can help to mitigate the erosion hazards, portending their development trend, and assist in developing a defense system **(Nassar *et al*., 2019)**.

Genz *et al*. (2007) defined the shoreline as the location of the land-water interface at a specific moment in time; this characteristic is extremely dynamic and serves as an indication for coastal erosion and accretion. Remote sensing and GIS techniques can be used to monitor a region's situation over time to identify changes that have occurred **(Abou Samra and El-Barbary, 2018; Hammad *et al*., 2022)**. A time series spectral data of different coastline locations is utilized to determine the rate of shoreline change statistics using the Digital Shoreline Analysis System (DSAS) extension tool. The U.S. Geological Survey's Coastal Change Hazards project included DSAS to supply a reliable suite of regression rates in a consistent and easily repeatable approach to run on vast amounts of data collected at multiple scales. The program is designed to aid in the computation of shoreline change and to provide rate of change information as well as arithmetical data required to ensure that the computed results are consistent **(Murali *et al*., 2013).**

DSAS is also suitable for any general application that involves calculating positional transformations over time, such as analyzing changes in glacier borders in chronological aerial images, river edge margins, or changes in land use/land-cover **(Thieler *et al*., 2009)**.

El-Alamein City is one of the newly constructed cities that need further investigation. Thus, the present study aims to assess water and sediment contamination of El-Alamein coast and inland lakes to assess environmental contamination and the vulnerability to erosion through mapping the shoreline in 2030 using DSAS, lab analyses and geostatistical techniques. Then a final degradation map will be produced

to assess the overall deterioration considering the erosion (actual and predicted) and the contamination in the area.

MATERIALS AND METHODS

1. Study area

The study area is represented by El-Alamein coastal zone, on Egypt's northwestern Mediterranean Sea coast, between latitudes 30º 42′ 30″ N to 30º 59′0″ N, and longitudes 28º 45′0″ E to 29º 12′0″ E (Fig 1). It's located in Matrouh Governorate and includes the villages of Sidi Abdel-Rahman and Tal El-Ais. El-Alamein was a tiny town with palm and olive trees before it became famous as a battleground. It is now one of the newly developed coastal locations, with a variety of activities such as recreational, commercial, and urban activities **(State Information Service, 2018; Hammad *et al.*, 2022)**.

The climate of the region is semiarid Mediterranean, with a short-wet winter and lengthy snug summer months (May to September) with clear skies, strong radiation, and no rain. An easterly longshore current is created by the prevalent wave directions (WNW, NW, and NNW) (from west to east). Longshore currents travel westward as waves approach from the N, NNE, and NE **(El-Banna and Hereher, 2009)**.

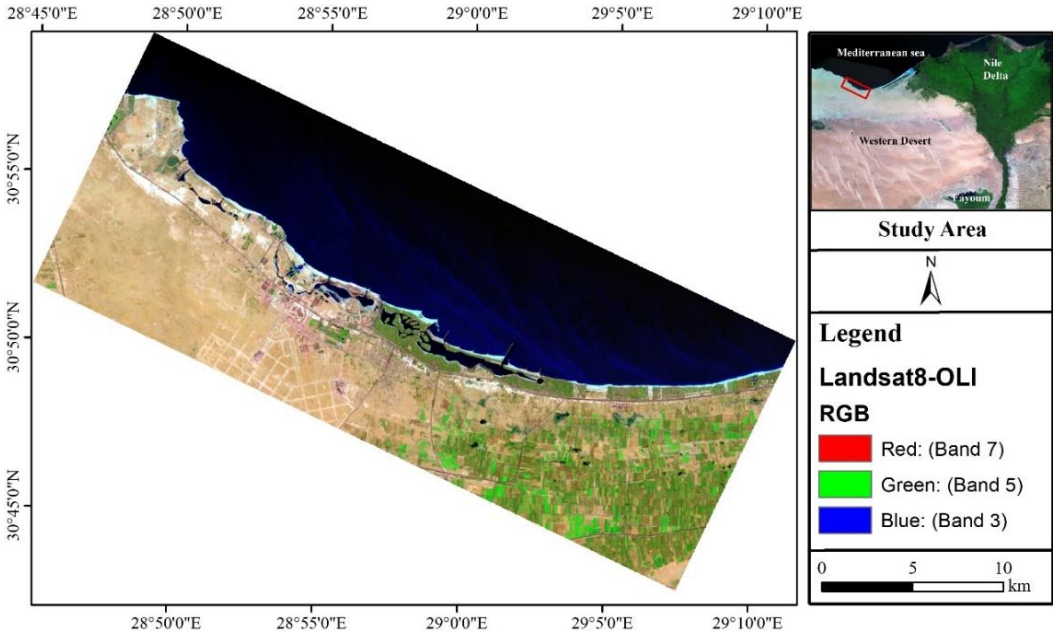

Fig (1). Study area location map.

2. Satellite Data Acquisition & Preprocessing

At first, three multispectral Landsat images (TM, ETM, and OLI) were freely downloaded for El-Alamein area on July 4th, 2000, July 8th, 2010, and July 19th, 2020, respectively. The U.S. Geological Survey generated the data collection, which was collected in geographic Tagged Image-File format (Geo TIFF). The data type is level 1, which is obtained from data provided by the sensor and spacecraft and offers

consistent radiometric and geometric accuracy. The study area was located in one scene (178-39) and was geometrically corrected to the universal transverse Mercator (UTM) Zone 35.

3. Assessing contamination in water and sediment

A total of 25 evenly spaced sites were used to collect water and sediment samples during November 13th and 14th, 2020 (Fig. 2). The pH, electric conductivity (EC) (ms/cm), turbidity (NTU), phosphate (PO_4) (mg/L), organic matter (OM), and four hazardous heavy metals (Pb, Cd, Ni & Fe) were all measured in the water. Also, the pH, EC, OM, and the same hazardous metals were measured in sediment using the Flame Atomic Absorption Spectrometer. The background values for the investigated heavy metals (Pb, Cd, Ni & Fe) were (20, 0.3, 68 & 47200 ppm), respectively. All water and sediment analyses followed the protocol of **APHA (1992).** The following metrics were used to assess the level of heavy metal contamination in sediment: contamination factor (CF), degree of contamination (DC), ecological risk (ER), ecological risk index (RI), enrichment factor (EF), pollution load index (PLI), and geo-accumulation index (Igeo). A list of these indices and categories being used in this study is illustrated in Table 1.

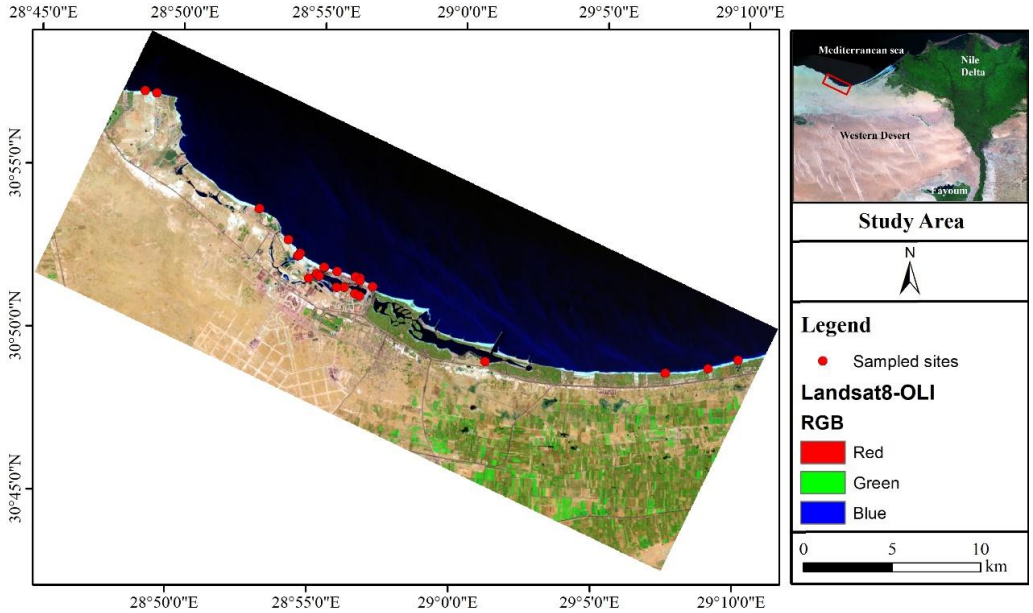

Fig. (2). All Sampled locations (Coastal and inland sites)

Table (1): Category of indices used to assess sediment pollution.

Index	Value	Category
CF	<1	Low contamination
	1 ≤ CF < 3	Moderate contamination
	3 ≤ CF < 6	Considerable degree of contamination
	CF ≥ 6	Very high contamination
Er	<40	Low potential ecological risk
	40 ≤ Er < 80	Moderate potential ecological risk
	80 ≤ Er < 160	Considerable potential ecological risk
	160 ≤ Er < 320	High potential ecological risk
	Er ≥ 320	Very high ecological risk
DC	n ≤ Dc < 2n	Low degree of contamination
	2n ≤ Dc < 4n	Moderate degree of contamination
	Dc > 4n	Very high degree
	< 150	Low ecological risk
RI	150 ≤ RI < 300	Moderate ecological risk
	300 ≤ RI < 600	Considerable ecological risk
	RI > 600	Very high ecological risk
	< 2	Deficiently to minimal enrichment
	2 ≤ EF < 5	Moderate enrichment
EF	5 ≤ EF < 20	Significant enrichment
	20 ≤ EF < 40	Very high enrichment
	≥ 40	Extremely high enrichment
PLI	< 1	No Pollution
	> 1	Polluted

3.1. Contamination factor (CF)

The degree of contamination is represented by the contamination factor (CF) **(Tomlinson *et al.*, 1980).** The CF is computed by dividing the quantity of each metal in sediment (C metal) by the background level (C background), which corresponds to the baseline values measured by **Turekian and Wedepohl (1961).** The distribution of elements in sedimentary rocks (shales) and the earth's crust were both used in the CF calculations.

CF = C metal /C background

where the CF< 1 denotes low contamination. 1 ≤ CF < 3 denotes moderate contamination, 3 ≤ CF ≤ 6 means significant contamination, while CF > 6 signifies extremely high contamination.

3.2. Degree of contamination (DC)

Another CF-based statistic is DC, which can be defined as the total of CFs for a specific location:

$$DC = \sum_{i=1}^{n} CF\,i$$

where n is the total number of elements.

3.3. Potential ecological risk index (RI)

The ecological risk of heavy metals in sediment was calculated using the prospective ecological risk index (RI) established as given in the equations below **(Hakanson, 1980)**.

$$RI = \sum_{1}^{n} Er$$

$$Er = Tr * CF$$

Because Er is a singular RI index, n is the number of heavy metals, and Tr is the toxic response factor for metals recommended by **Hakanson**.

3.4. Enrichment factor (EF)

A well-known technique for assessing the impact of human activity on sediments is the computation of a normalized enrichment factor (EF) for metal concentrations over uncontaminated baseline values **(Salomons and Förstner, 1984; Hornung *et al.*, 1989; Dickinson *et al.*, 1996)**. EF was used in the present study because the EF computation is a valuable method for visualizing geochemical trends across large geographic regions with considerable mud (i.e., clay rich) to sand ratio variations and aims to reduce metal variability associated with mud/sand ratio variations. The EF method calibrates measurements of heavy metal concentrations against a sample reference metal, such as Fe or Al **(Ravichandran *et al.*, 1995)**. In this method, the Fe or Al is employed as a "proxy" for the clay component **(Windom *et al.*, 1989; Din, 1992)**. In a study of marine sediment near Christchurch, **Stewart (1989)** used a similar technique and used Mn for EF computations. Because other heavy elements were not linked to the Fe distribution, according to **Deely and Fergusson (1994)**, they suggested Fe as a suitable normalizing element to be incorporated into the enrichment factor computation. Fe has a relatively high natural content, thus anthropogenic sources are unlikely to considerably increase it in estuarine sediments **(Niencheski *et al.*, 1994)**. Fe and Al normalization have been utilized as a substitute to grain size normalization in a variety of research **(Bruland *et al.*, 1974; Windom *et al.*, 1989; Bresline and Sanudo-Wilhelmy, 1999).** In modern sediments from estuaries of Texas, **Sharma *et al.* (1999)** employed Al and Fe together to identify natural and human sources. Cobalt (Co) was recently added as a normalizing element for detecting human contamination causes in coastal sediments of Sydney, Australia **(Matthai and Birch, 2001).**

The following equation is used to compute the EF:

$$EF = Mx \; X \; Feb \; / Mb \; X \; Fex$$

where Mx and Fex are concentrations of the metal and Fe (or other normalizing element) values in sediment sample, and Mb and Feb are their amounts in a baseline reference material or an appropriate background **(Salomons and Förstner, 1984)**.

3.5. Pollution load index (PLI)

The metal contamination degree at each site was determined using the following approach using the pollution load index (PLI) proposed by **Thomson *et al.* (1980)**:

$$PLI = (CF_1 * CF_2 * CF_3 * CF_4 * \ldots * CF_n)^{1/n}$$

where n is the no. of metals investigated (in the present case will be four) and CF denotes the contamination factor. The PLI is a simple yet comparable method of measuring site fineness, with a value of PLI < 1 denoting perfection, PLI = 1 denoting baseline levels of contaminants, and PLI > 1 denoting site quality deterioration **(Thomilson *et al*., 1980)**.

3.6. Geoaccumulation index (Igeo)

Calculating the geo-accumulation index (Igeo) suggested by **Müller (1969)** is a typical technique for measuring the content of metal concentrations over background values. On basis of the rising numerical values of the indicator, the technique classifies metal pollution into seven enrichment groups (Table 2). The following equation is used to compute this index:

$$Igeo = log_2 C_n / 1.5\ B_n$$

where Cn is the element's content in the enriched samples and Bn is the element's background value. Also, the factor 1.5 is used to reduce the impact of any fluctuations in baseline values because of lithologic differences in the sediments **(Stoffers *et al*., 1986).**

For the growing Igeo values, **Müller (1969)** provided the following descriptive classification:

Table (2): Different classes of Igeo used in the present study

Igeo value	Igeo class	Designation of sediment quality
>5	6	extremely contaminated
4–5	5	strongly to extremely contaminated
3–4	4	strongly contaminated
2–3	3	moderately to strongly contaminated
1–2	2	moderately contaminated
0–1	1	uncontaminated to moderately contaminated
0	0	uncontaminated

4. Geostatistical analyses

Using ArcGIS 10.5, the geographic position of each visited location was recorded and transformed into a GIS ready layer that was associated with the laboratory analyses. Then, by using Inverse Distance Weighing (IDW) in geo-statistical studies were carried out. Maps of spatial distribution of water and sediment properties for every parameter were created as raster layers. Water and sediment parameters in El-Alamein region were mapped using the integrated spatial and non-spatial data sets. Non-spatial data were represented by detailed analyses, each of which had its own ID. The geographic location of each collected water and sediment sample was used to generate spatial data sets. Inverse Distance Weighing (IDW) was used to perform geostatistical analysis and map water and sediment properties/ all relevant contamination indices.

5. DSAS tool for monitoring shoreline changes

The impacts of anthropogenic activities on El-Alamein region coastline were quantified using DSAS version 5.0 during a 20-year period (2000–2020). DSAS is a

free tool added to ESRI ArcGIS v.10.5 that uses vector data to produce change rate statistics from several old shoreline points **(Thieler *et al*., 2009).** The 1st step in using DSAS to analyze data is to build a baseline parallel to the coastline from which transects will emerge perpendicularly. The 2nd step is to set transect parameters that divide the coastline into intervals and the 3rd step is to set and calculate change rate statistics at every transect **(Emam and Soliman, 2020; Baig *et al*., 2020).** The multi-date shorelines (1990–1995–2000–2010–2020) were digitized as shapefiles from satellite images of various time periods and used as input in the (DSAS) technology to compute and predict the shoreline erosion in 2030.

RESULTS & DISCUSSIONS

1. Spatial analyses and assessment of water and sediment characteristics

Tables 3 and 4 show the statistics of the investigated water and sediment quality characteristics in El-Alamein region including the samples collected from the Mediterranean Sea and the inland ponds.

Table (3): Water and sediment analyses statistics.

Water statistics	**pH**	**Conductivity (ms/cm)**	**Organic Matter %(w/v)**	**Pb (mg/L)**	**Cd (mg/L)**	**Ni (mg/L)**	**Fe (mg/L)**	**Turbidity (NTU)**	**PO4 (mg/L)**
Minimum	7.90	56.20	0.78	0.51	0.06	0.32	0.25	0.70	ND
Maximum	8.60	128.20	2.34	1.02	0.17	1.20	1.94	20.60	ND
Mean	8.35	79.42	1.26	0.71	0.10	0.64	0.64	6.30	ND
S.D.	0.19	25.05	0.52	0.16	0.04	0.30	0.44	4.30	ND
Sediment statistics	**pH**	**Conductivity (ms/cm)**	**Organic Matter %(w/w)**	**Pb (mg/kg)**	**Cd (mg/kg)**	**Ni (mg/kg)**	**Fe (mg/kg)**	**_**	**_**
Minimum	8.70	0.78	1.45	19.19	1.68	9.60	720.95	_	_
Maximum	9.60	3.77	6.64	37.99	3.51	16.82	2518.95	_	_
Mean	9.30	1.64	2.57	30.35	2.90	14.54	1189.72	_	_
S.D.	0.27	0.95	1.26	4.40	0.48	1.65	540.60	_	_

Table (4): Sediment samples mechanical analyses statistics.

Statistics	**Grain %**	**Sand %**	**Silt %**	**Clay %**	**Skewness (SkI)**	**Kurtosis (KG)**
Minimum	0	53.64	0	0	0.01	0.04
Maximum	44.27	100	7.76	6.44	0.39	1.64
Mean	5.63	92.63	1.14	0.6	0.14	0.75
S.D.	11.43	12.66	2.06	1.46	0.11	0.54

A. Water pH

In the research region, weak alkaline samples of water were found, particularly in the middle part, where pH extended from 7.9 to 8.6, with a mean of 8.35 and a standard deviation of 0.19 (Fig. 3) which might indicate a pH-friendly environment. The pH spatial distribution in water samples increases from the center to the east and west, with the most alkaline water found in the research area's eastern and western regions. The **EPA (2017)** advised a pH range of 6.5–8.5 for aquatic life protection, which was slightly surpassed in the water of the research area' eastern and western regions. For water samples, eastern of the research region indicated an alkaline pH (7.74–9.82) **(Elnazer and Salman, 2021)**.

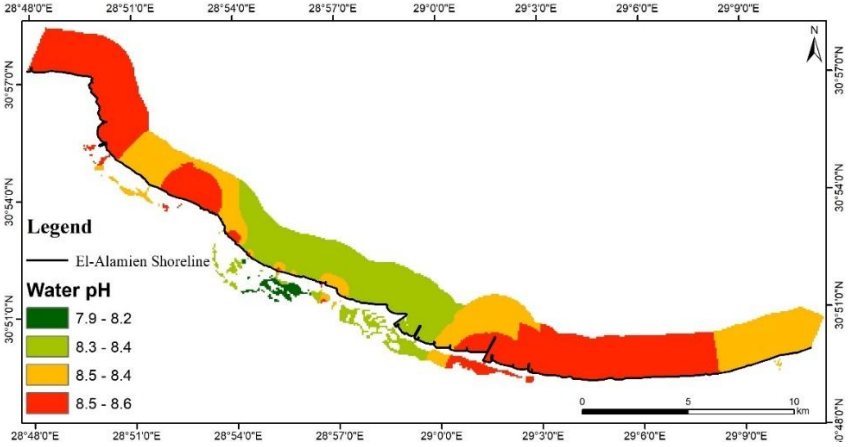

Fig (3): Spatial distribution map for levels of pH in water.

B. Water electric conductivity (mS/cm)

The EC of water samples varied greatly from the lowest values in east and west to the highest levels in the center, near the building zone of the new El-Alamein towers (Figs. 4). Water had an EC of 56.2 to 128.2 mS/cm, with a mean of 79.42 mS/cm and a standard deviation of 25.05 mS/cm.

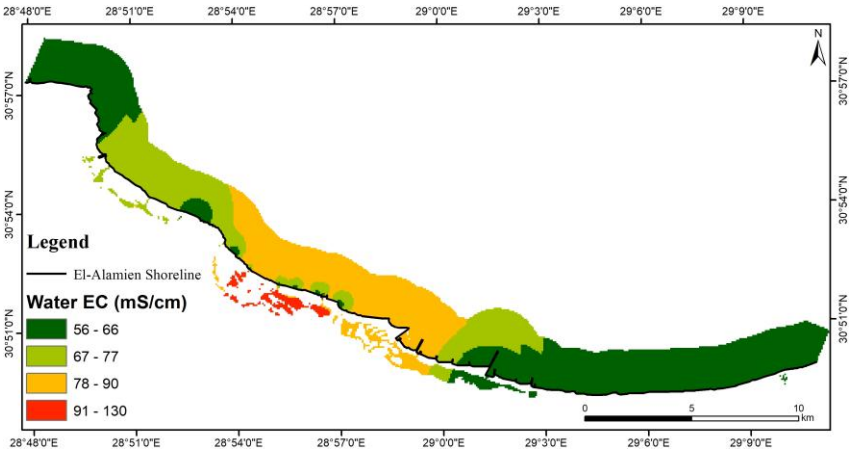

Fig (4): Spatial distribution map for levels of EC in water.

C. Water turbidity (NTU)

The turbidity of water varied spatially similar to EC patterns, ranging from 0.7 to 20.6 NTU with a mean value of 6.3 NTU and a standard deviation (S.D) of 4.3 NTU, with the greatest values (5.21–20.6 NTU) in the middle of the study region near the location where the new El-Alamein towers are found (Fig. 5). High turbidity levels at these sites might be due to residuals from building activities.

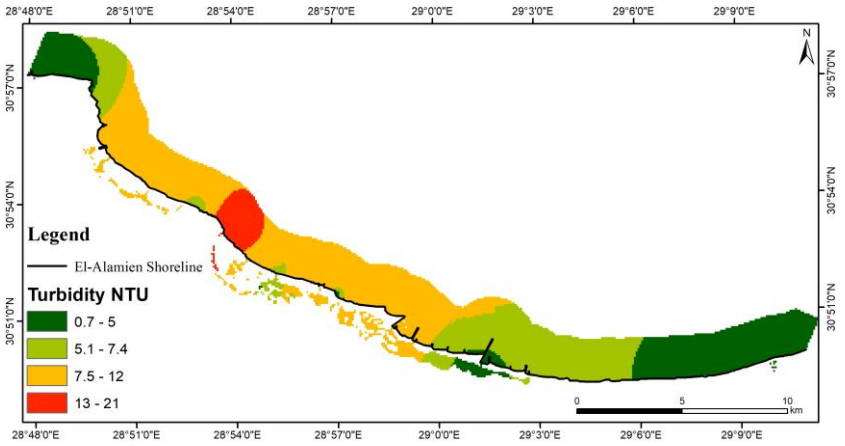

Fig (5): Spatial distribution map for Turbidity of water samples.

D. Water organic matter (w/v%)

Furthermore, the greatest amounts of organic matter (OM) in water were found in the same location (i.e., the middle of the research area) ranging from 1.09% to 2.34%. This reflects the significant organic load in this location, owing to nearby anthropogenic activity. The concentration of OM in water varied from 0.78% to 2.34%, with a mean of 1.26% and S.D of 0.52% (Fig. 6). **El-Zeiny *et al*. (2019)** referred to the same relation between turbidity and OM in Qaroun Lake because OM in water participated in higher levels of turbidity, a positive correlation between turbidity of water and OM concentration was observed (0.465).

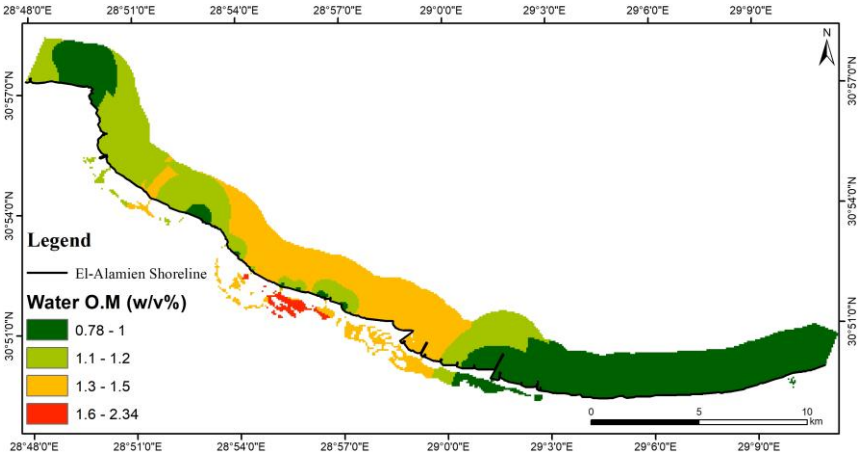

Fig (6): Spatial distribution map for Organic Matter in water.

E. Phosphate (PO_4)

The phosphate is not detected around the whole area; this can be explained by the absence of sewage and agricultural drainage in the study area. **El-Rayis *et al.* (2012)** also found that the average total phosphate (TP) concentration in Alamein Marina Lagoon throughout the study period (2007-2008) was 0.5 mg/l (0.47 mg/l for the surface samples and 0.68 mg/l for bottom samples), indicating a state of unproductive and unpolluted water of the lagoon.

F. Sediment pH

In the research region, weak alkaline sediment samples were found, particularly in the center, where pH varied from 8.7 to 9.6, with a mean of 9.3 and S.D of 0.27 (Fig. 7). The most alkaline sediments were in the eastern and western regions of the research area. The spatial distribution of pH in sediment samples increases from the middle to the east and west. **Elnazer et al. (2015)** reported that sediment samples' pH analyses ranged from 7.3 to 8.7, with half of the samples having pH values between 7.7 and 8.4. They found that it was of a moderately alkaline to alkaline nature and didn't vary considerably along the roadside of the Alexandria-Marsa Matruh route.

The reactivity of the soils investigated by **Elnazer and Salman (2021)** was alkaline, with pH rising from 7.93 to 8.72, low organic matter (0.52%), and a sandy composition. These features are mentioned as the soil's marine nature and the research area's aridity. The soil was mostly originated from the extensive carbonate rocks weathering in the study area's southern region.

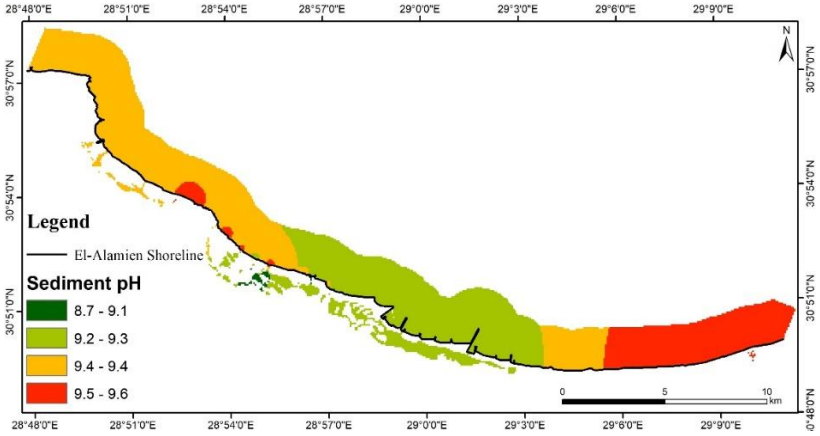

Fig (7): Spatial distribution map for levels of pH in sediment.

G. Sediment electric conductivity (mS/cm)

The EC of sediment samples indicated a wide spatial variation, extending from the lowest levels in the research area's east and west to the highest values in the center of study region, near the site of the new El-Alamein towers' construction (Fig. 8). EC of sediment ranged from 0.78 to 3.77 with mean of 1.64 mS/cm and S.D of 0.95 mS/cm.

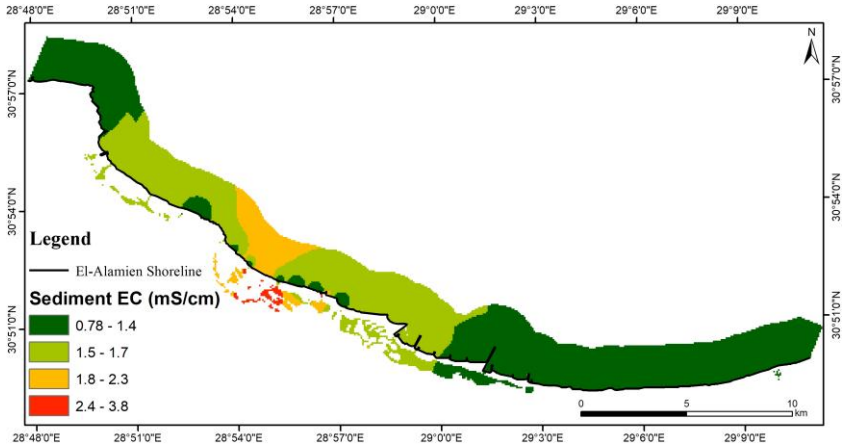

Fig (8): Spatial distribution map for levels of EC in sediment.

H. Sediment organic matter (w/w%)

Organic matter levels in bottom sediments vary greatly (1.45–6.64%), with a mean of 2.57% and S.D of 1.26%, and higher levels of organic matter accumulate in bottom sediments, particularly in the midsection (Fig. 9).

This reflects the significant organic load in this location, owing to nearby anthropogenic activities. **Elnazer *et al*. (2015)** discovered that the OM content of the sediment is low, with maximum of 2.07%, and 75% of samples having OM less than 1%. When compared to fair soils, the soil near the road includes a higher percentage of OM. This might be due to fuel combustion deposition, tire wear, and oil leaks.

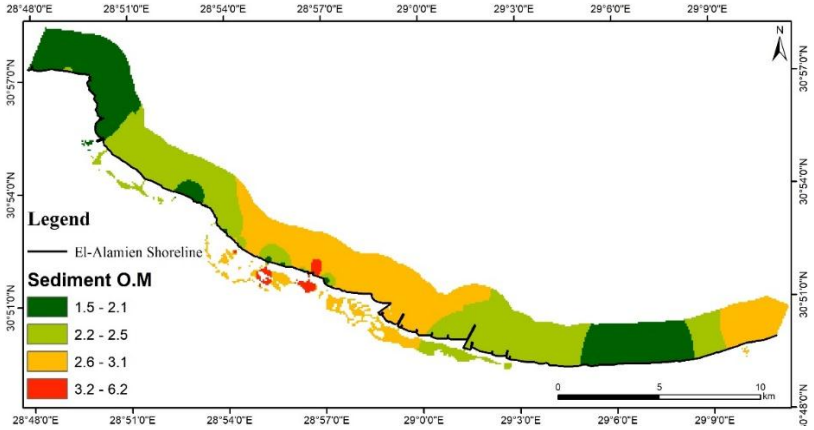

Fig (9): Spatial distribution map for Organic Matter (%) in sediment.

2. Spatial patterns of heavy metals in water and sediment samples.

In water samples of the research region, 4 hazardous heavy metals were tested in this investigation. The spatial distributions of the metals analyzed in water are illustrated in figures (10–13). Fe and Ni were the most common metals found in the research area's water. Fe levels varied from 0.25 to 1.94 mg/l, with a mean of 0.64 mg/l and a standard deviation of 0.44 mg/l. Ni levels varied from 0.32 to 1.2 mg/l, with a mean of 0.64 mg/l and S.D of 0.3 mg/l. Both metals had a similar geographical distribution in water, with levels increasing in the middle, whereas in sediment Fe increases from middle to west while Ni increases along the study area's shore.

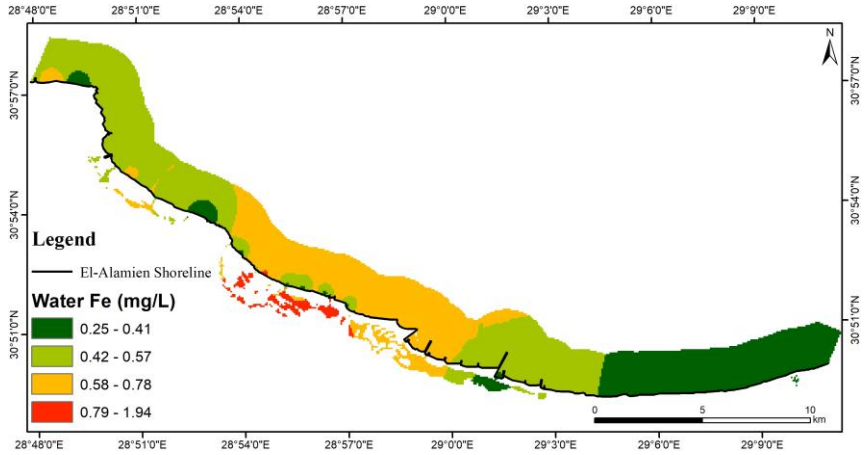

Fig (10): Spatial distribution map for Fe in water.

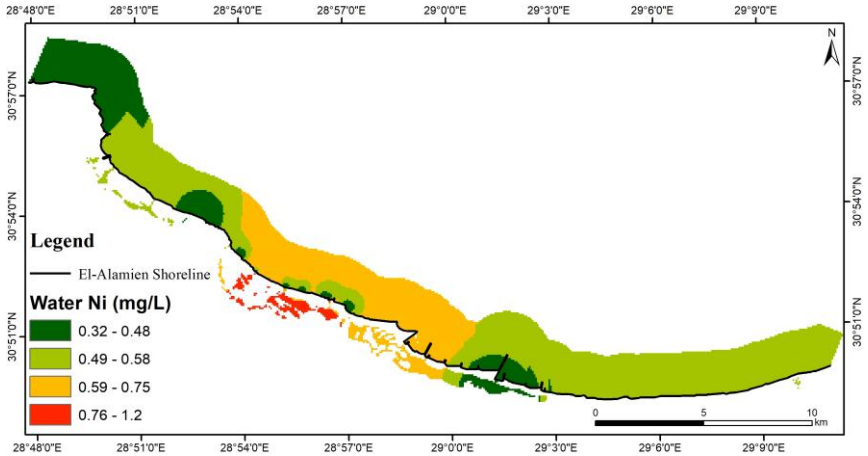

Fig (11): Spatial distribution map for Ni in water.

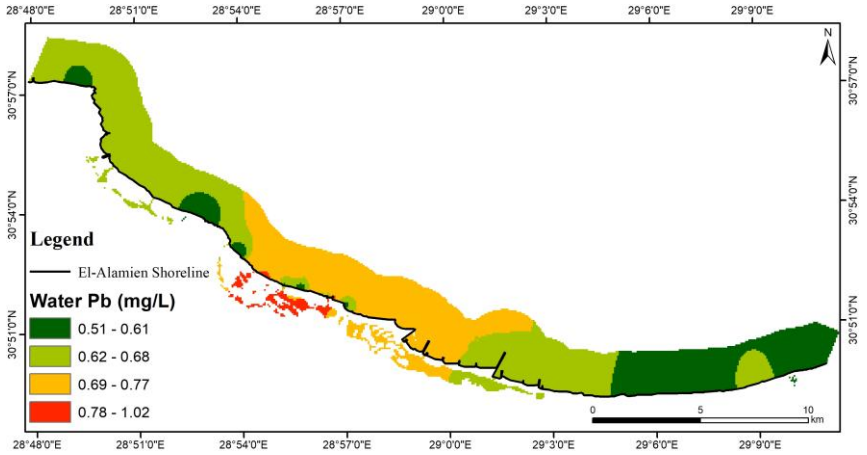

Fig (12): Spatial distribution map for Pb in water.

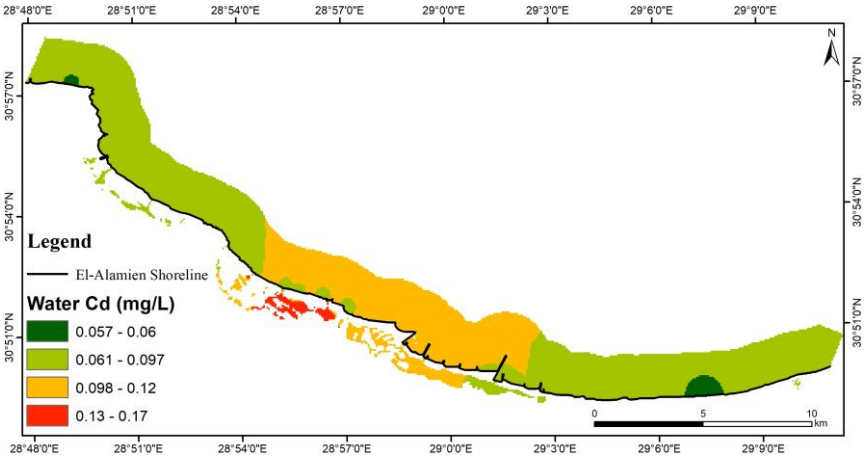

Fig (13): Spatial distribution map for Cd in water.

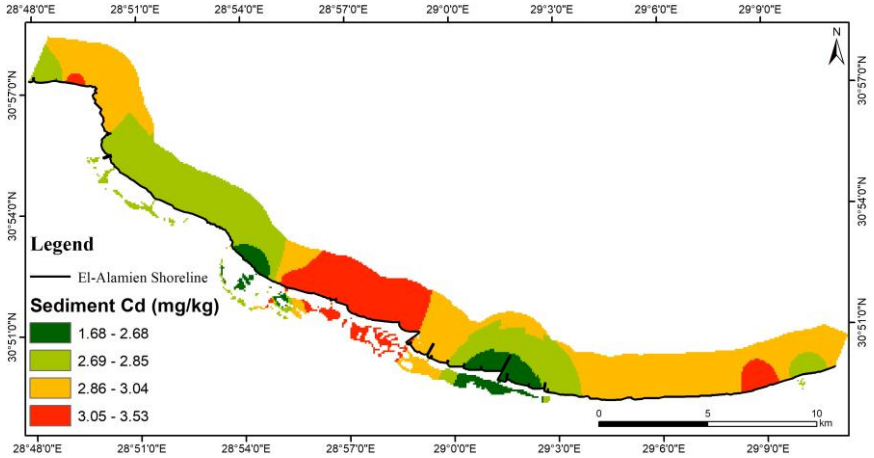

Fig (14): Spatial distribution map for Cd in sediment.

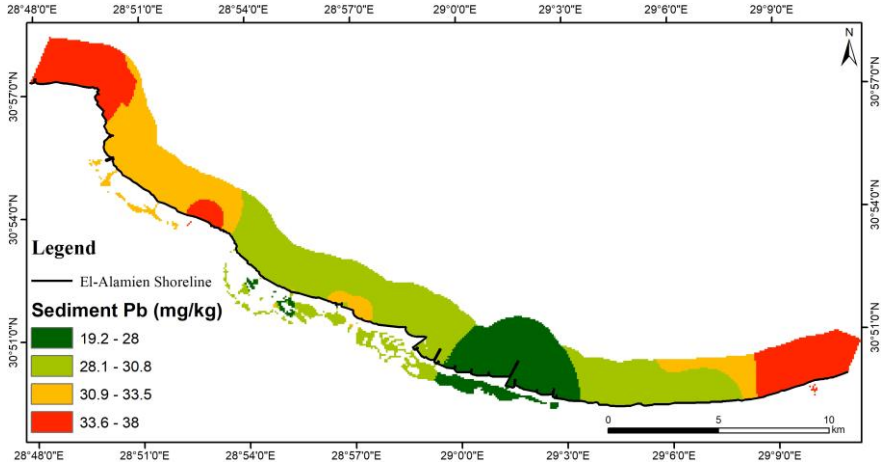

Fig (15): Spatial distribution map for Pb in sediment.

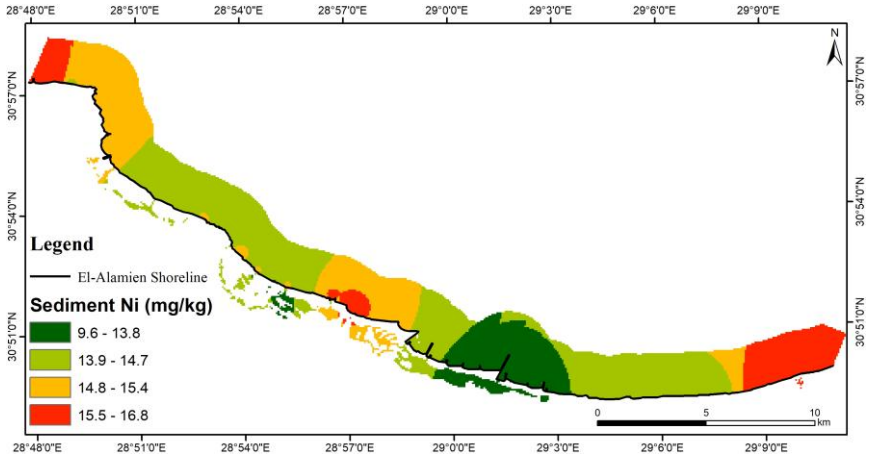

Fig (16): Spatial distribution map for Ni in sediment.

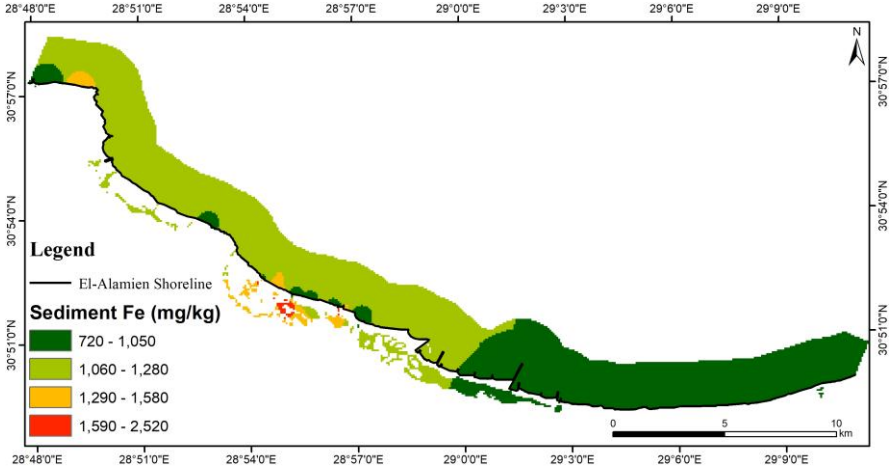

Fig (17): Spatial distribution map for Fe in sediment.

Pb and Cd levels in water were found to be lower in comparison to Fe and Ni levels. Cd levels varied from 0.06 to 0.17 mg/l, with a mean of 0.1 mg/l and S.D of 0.4 mg/l. Pb levels fluctuated from 0.51 to 1.02 mg/l, with a mean of 0.71 mg/l and S.D of 0.16 mg/l. Pb had an analogous spatial distribution to Ni, but Cd had a different spatial distribution since its high levels in water were found in the intermediate area, particularly in the artificial ponds near the new constructions. Some metals (e.g., mercury, cadmium, and lead) are hazardous even at extremely low doses with no biological importance **(Zheng *et al*., 2015)**. **Elnazer and Salman (2021)**, discovered that the water of El Hammam canal, which is located to the east of the research region, had an unsatisfactory concentration of Cd and Ni with average concentration of 25.3 μg/l and 280.8 μg/l, respectively.

The regional patterns of the four hazardous metals examined in bottom sediments are illustrated in figures (14–17). The investigated metals were found in significant concentrations in the bottom sediments. The concentration of Cd in sediments varied from 1.68 to 3.53 mg/kg, with an average of 2.9 mg/kg and S.D of 0.48 mg/kg. **Elnazer *et al*. (2015),** deduced that Cd levels in soils started from 1.25 to 3.15 μg/g, and that P-fertilizers and deposition of vehicle exhaust are sources of Cd in soils, whereas phosphatic deposits in Egypt that are utilized in super phosphate fertilizers include 20 μg/g Cd **(El Kammar, 1974)**. Given the absence of industry in the surveyed locations, the amounts of Cd might be attributable to oils of lubrication and tire wear, with Cd levels in automobile tires ranging from 20 to 90 μg/g **(Nan *et al*., 2006)**. Long-term cadmium exposure can harm the neurological system, liver, and cardiovascular system, as well as cause kidney dysfunction and death in animals and mammals **(Semerjian, 2010)**.

The greatest metals concentration in sediments were for Pb and Ni, showing a great fluctuation which ranged from 19.19 mg/kg to 37.99 mg/kg with a mean of 30.35 mg/kg and S.D of 4.4 mg/kg for Pb, and from 9.6 mg/kg to 16.82 mg/kg with a mean of 14.54 mg/kg and S.D of 1.65 mg/kg for Ni.

Elnazer *et al*. (2015), discovered that total Pb concentration varied from 29.15 to 50.6 μg/g (greater than the range in the El-Alamein region under investigation), and that the amount of Pb in soil is reduced as space from the road is increased. The high intensity along the road refers that vehicle exhaust has a role, as does the usage of gasoline anti-knock additives made of alkyl-lead compounds **(Gratani *et al*., 1992)**. Lead is extremely harmful to human health. It may cause reduction in intelligence level, hyperactivity, and sound deafness in children, as well as high blood pressure level, liver, kidney, and damage to fertility in adults **(Okorie, 2010)**.

Fe levels varied greatly as they ranged from 720.95 to 2518.95 mg/kg, with a mean of 1189.72 mg/kg and a standard deviation of 540.60 mg/kg.

3. Heavy Metal Contamination Risk Assessment

The Contamination Factor (CF), which analyses the reference levels of harmful metals in the environment (Shale of the earth), may be used to define the spatial distribution of these metals. This parameter evaluates the level of sediment samples contamination caused by every metal separately **(El-Zeiny *et al*, 2019).** The CF revealed that the research area' sediments are heavily polluted with Pb and Cd metals. In the case of Cd, one contamination level was recorded: very high contamination. Most of the research area is heavily contaminated with Cd (Fig. 18). The second pollutant identified by the CF was Pb that had a moderate level of contamination (Fig. 19).

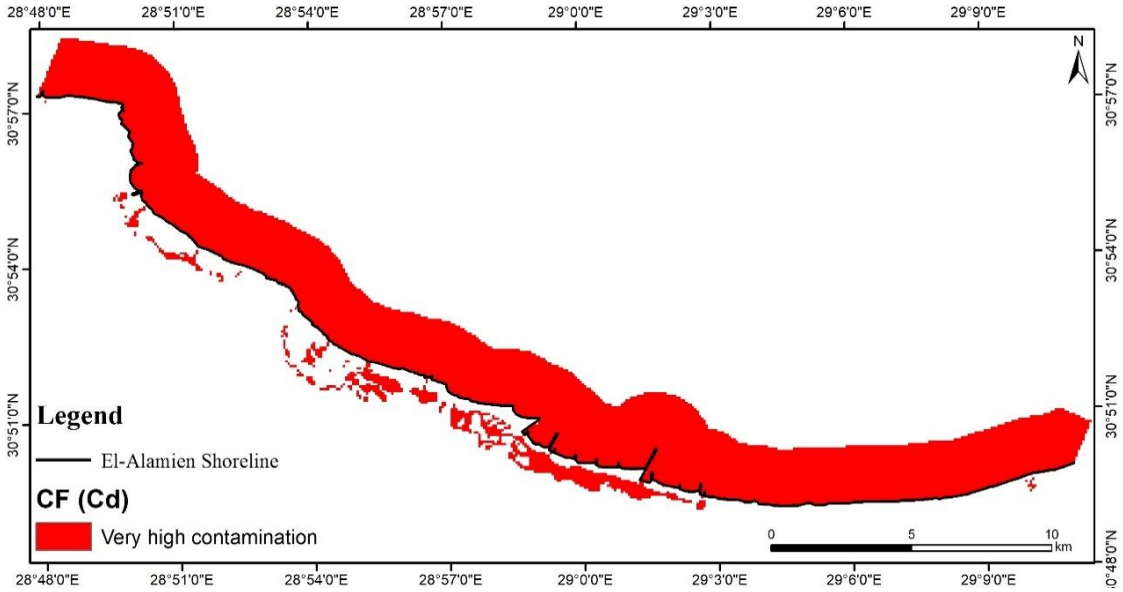

Fig (18): Spatial distribution map for CF of the Cd in sediment.

Elnazer *et al*. (2015) found that the CF values was >1 for Pb and Cd, the majority of the samples (approximately 85%) had significant CF for Cd, while the remainder have moderate CF and all the samples have moderate CF for Pb. This is consistent with the present study (Fig. 19). These findings point to possible contamination, particularly with regard to the dangers of Pb and Cd. Fe and Ni, however, revealed low contamination over the whole region (Figs. 20nd 21).

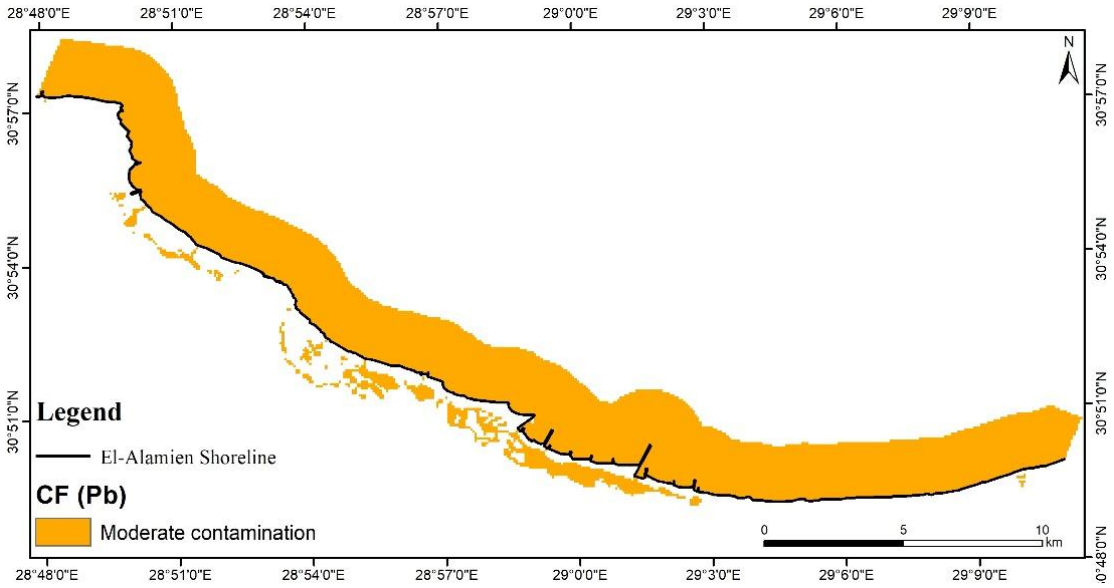

Fig (19): Spatial distribution map for CF of the Pb in sediment.

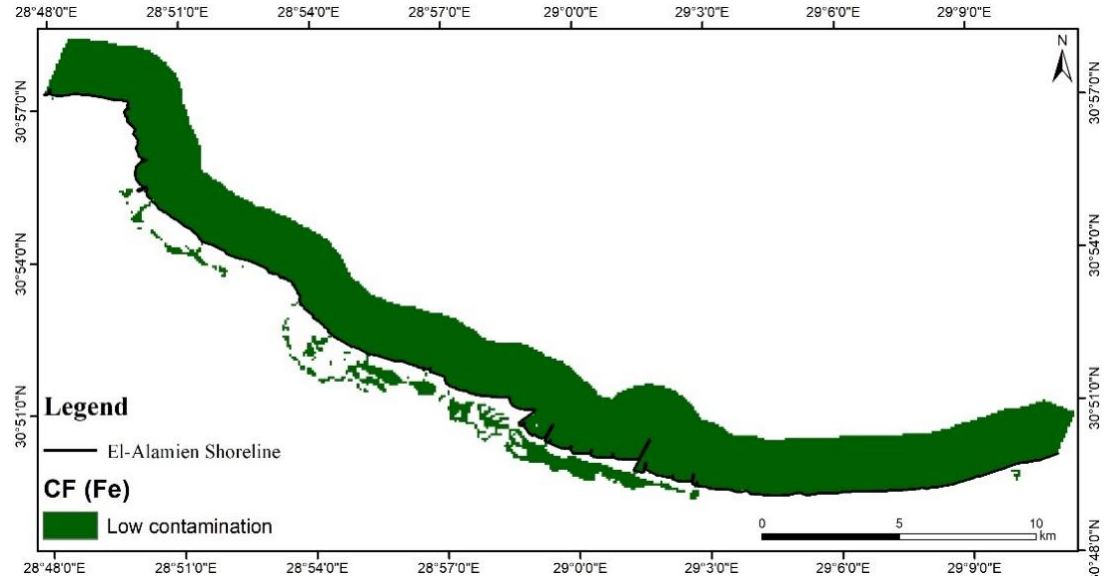

Fig (20): Spatial distribution map for CF of the Fe in sediment.

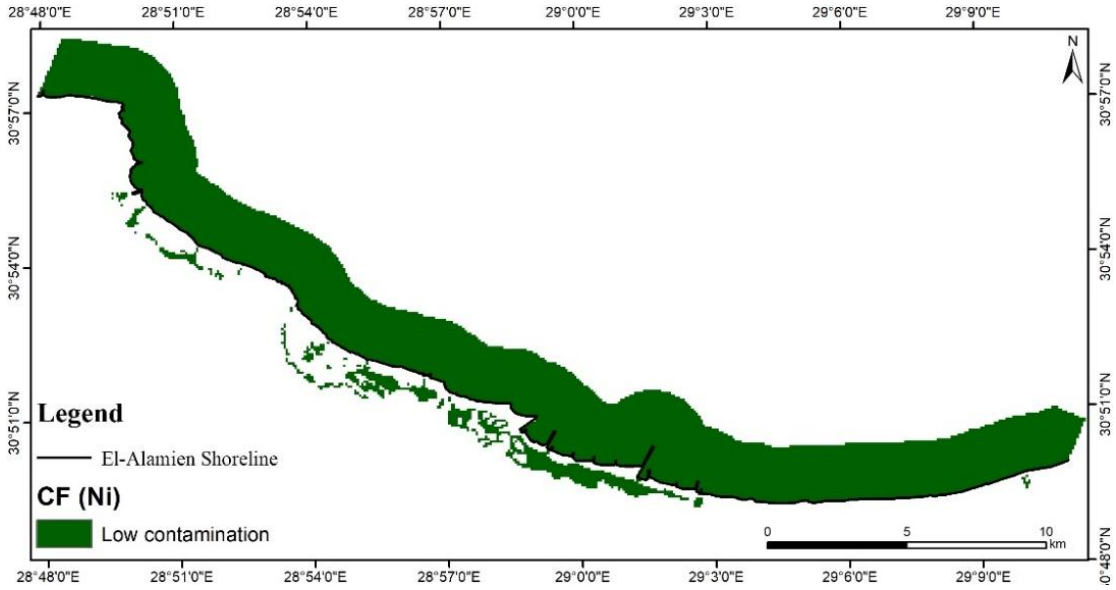

Fig (21): Spatial distribution map for CF of the Ni in sediment.

The contamination degree (DC) map was created to measure the total degree of hazardous metal contamination in sediment (Fig. 22). The DC displayed the sediments' cumulative level, showing low and moderate level of contamination. The ecological risk map assesses the impact of this contamination on the ecosystem.

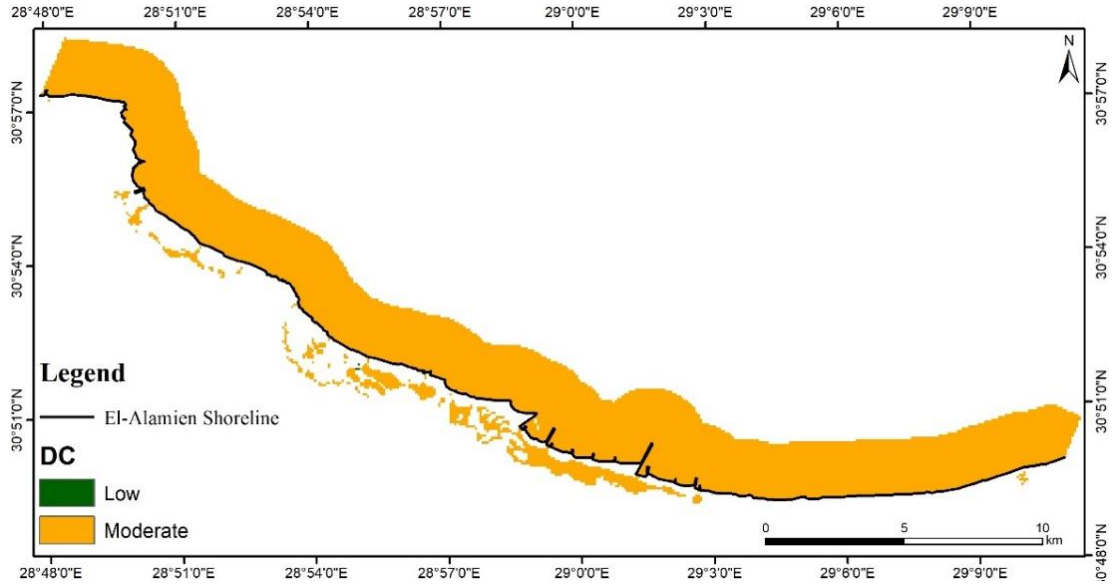

Fig (22): Spatial distribution map for DC of the toxic metals in sediment.

The Er maps (Figs. 23-25) revealed that the area's sediment pollution resulted in three categories of risk: low, high, and very high. The ecological danger is moderately affecting majority of the region. The low Er was due to Ni, whereas the high and very high ecological risk zones were due to Cd levels. **Elnazer *et al.* (2015)** discovered that the computed Er revealed that Pb poses a small risk to the local aquatic life, however Cd

had the greatest Er, ranging from considerable to high risk, implying that the ecological risk is mostly due to Cd soil pollution.

Elnazer and Salman (2021) discovered that the investigated soil samples had no biological risk of Pb (15 samples), moderate and significant (Er) from the presence of Ni in certain samples, while Cd levels were very high (Er).

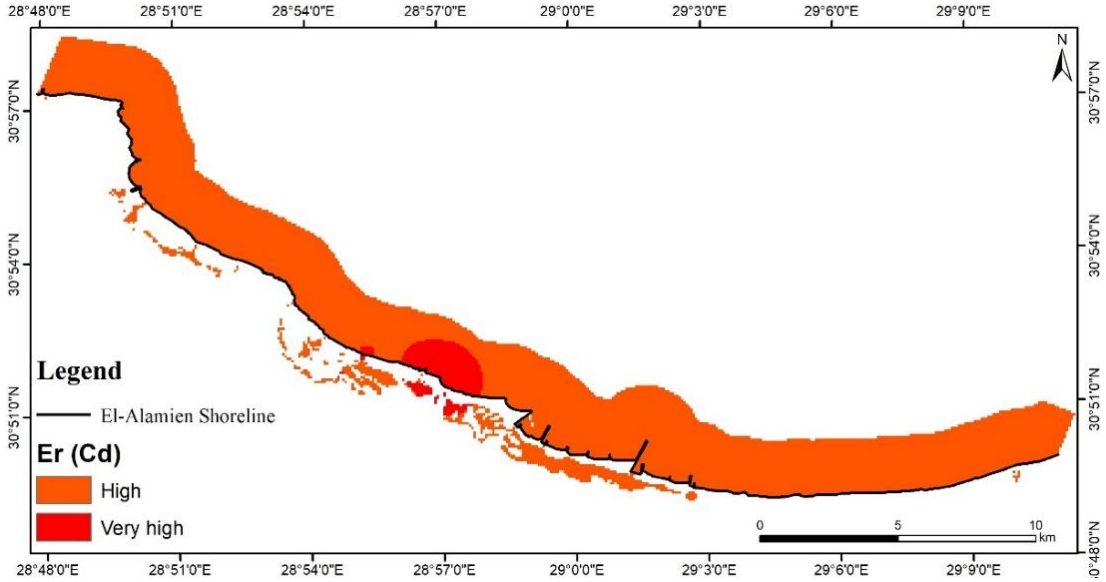

Fig (23): Spatial distribution map for Er of the Cd in sediment.

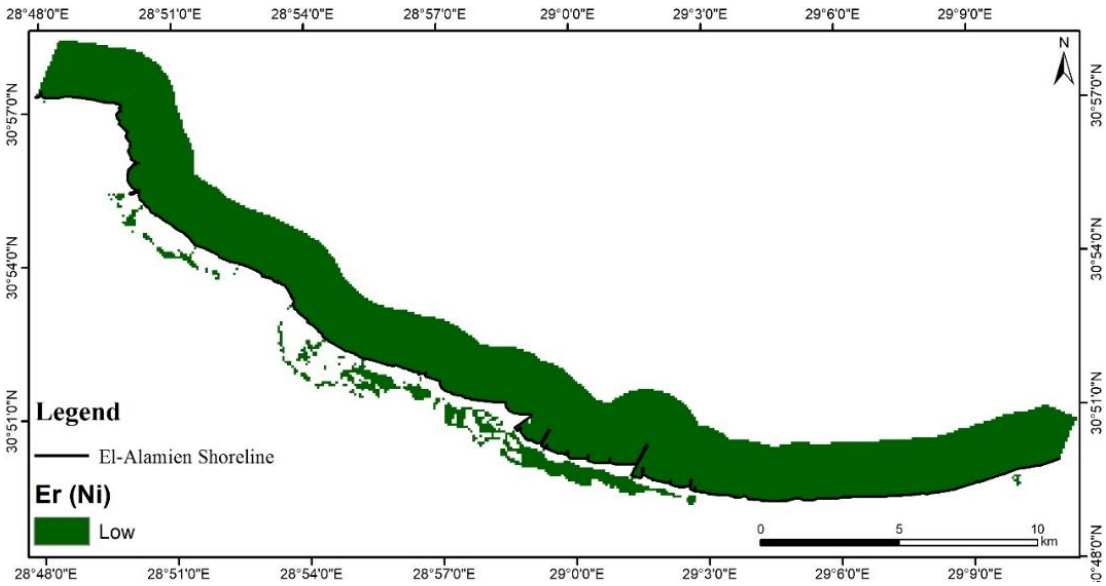

Fig (24): Spatial distribution map for Er of the Ni in sediment.

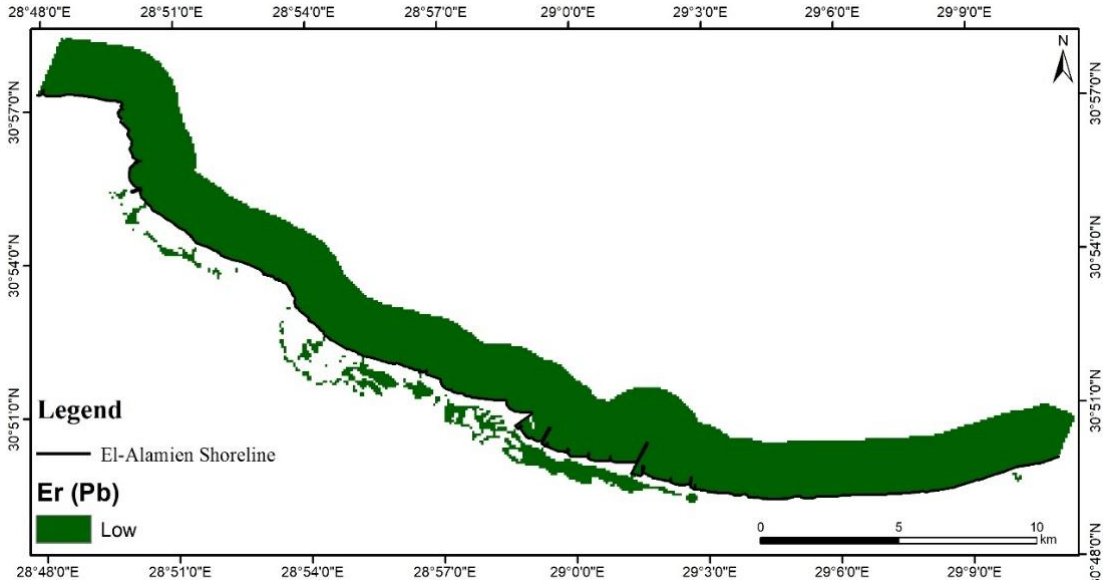

Fig (25): Spatial distribution map for Er of the Pb in sediment.

As demonstrated in (Fig. 26), the potential ecological risk in the research region is quite low throughout the whole area. **Elnazer *et al*. (2015)** deduced that the total potential ecological risk in the metals identified in (62 %) of the tested sediment is low, with RI < 150. The remaining samples (38%) had a moderate RI.

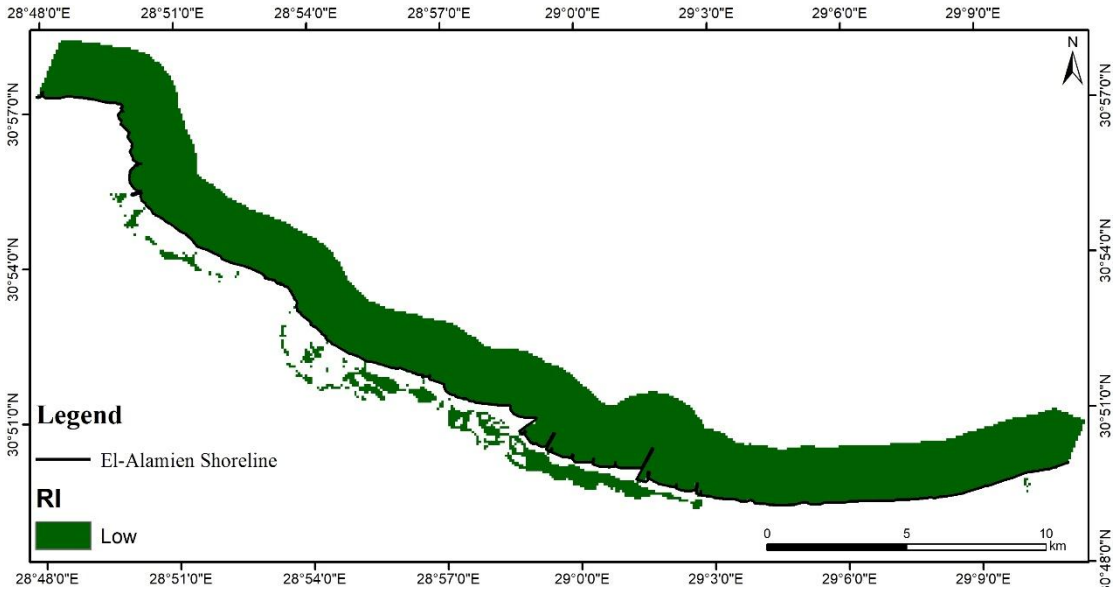

Fig (26): Spatial distribution map for Risk Index in sediment.

According to **Elnazer and Salman (2021)** at eastern of El-Alamein study area, they found that the (RI) revealed that the majority of the investigated sites (15 sites) had a very high RI, while five (5) have a considerable RI. Cd is the predominant cause of the high RI, followed by Ni to a lesser extent.

The enrichment factor percent changes accordingly with the metal under study since the EF of Cd is extremely high along the whole area shoreline (Fig 27).

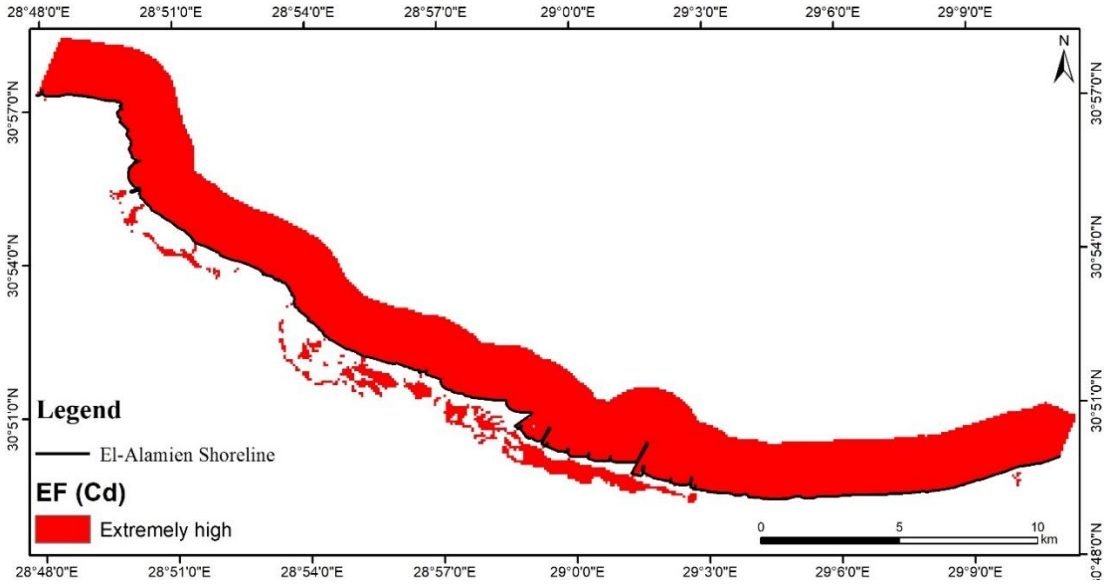

Fig (27): Spatial distribution map for EF of Cd in sediment

However, throughout the research area's beach, the EF of Ni varies from moderate to significant (Fig 28). Furthermore, the EF of the Pb is very high along the research area's and increased to extremely high levels (Fig 29).

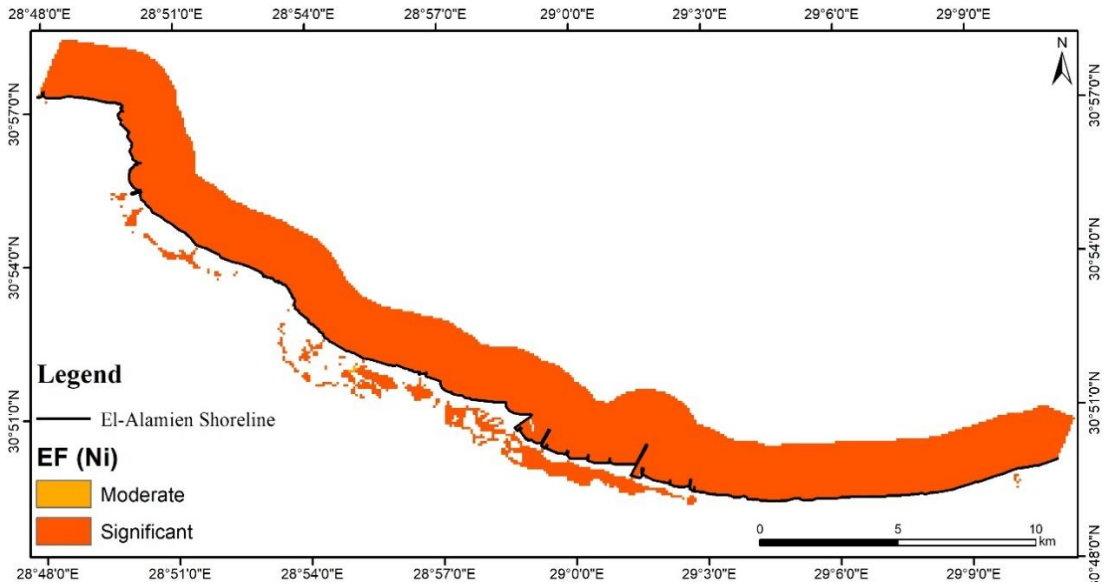

Fig (28): Spatial distribution map for EF of Ni in sediment

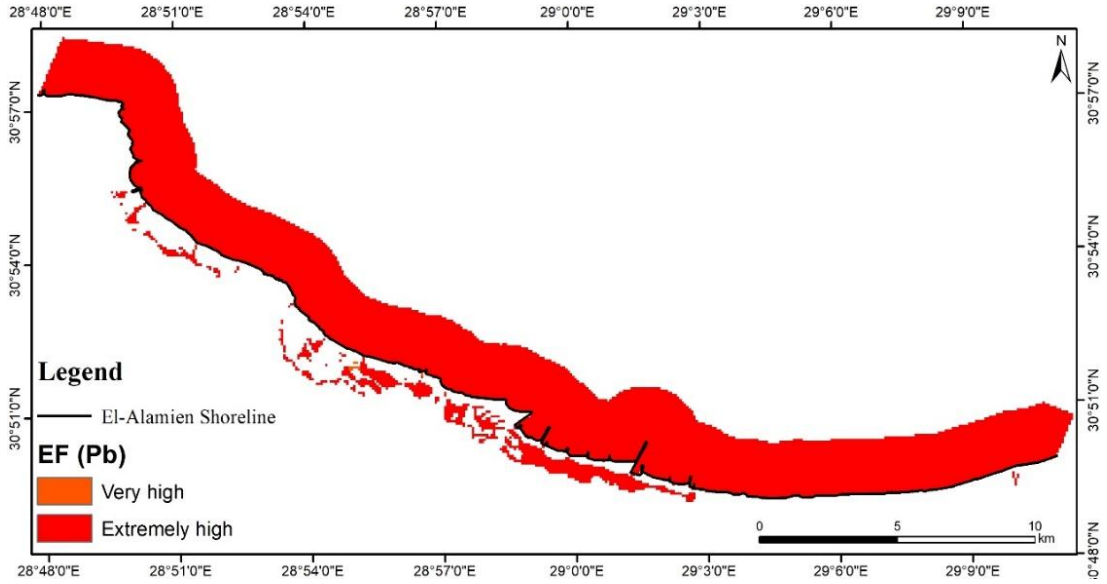

Fig (29): Spatial distribution map for EF of Pb in sediment

The (PLI) values in the study region indicate that there is no pollution throughout the whole study area's shore with values <1 (Fig 30). However, **Elnazer *et al.* (2015)** deduced that PLI results for all of samples are >1, indicating the importance of discrete external sources of sediment pollution, such as car exhaust and agricultural operations.

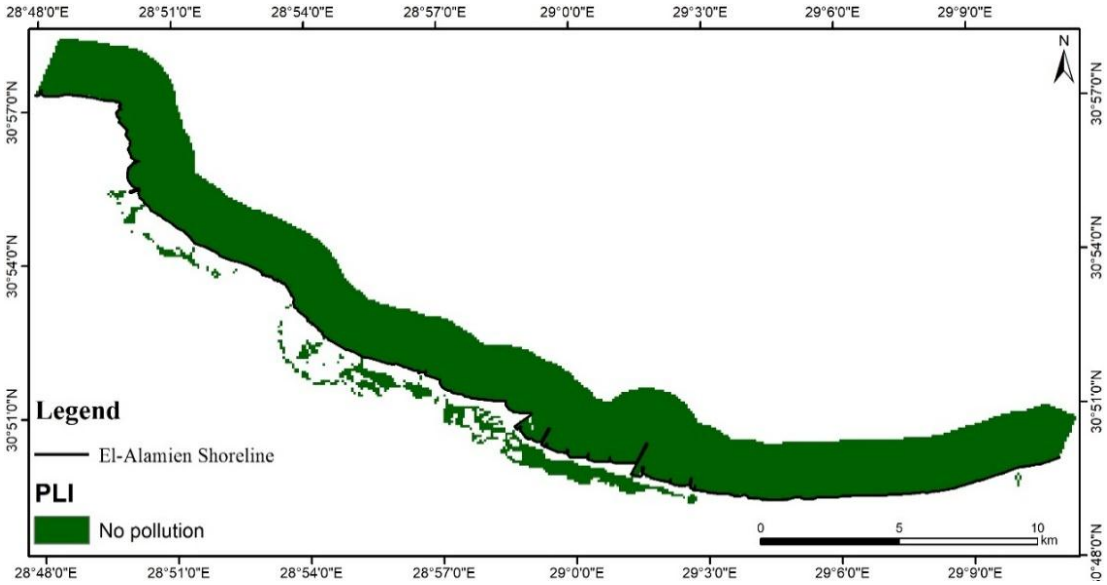

Fig (30): Spatial distribution map for PLI in sediment

The (Igeo) values computed are displayed in (Fig 31-34). The Igeo readings show that the region is substantially contaminated with Cd, but not with Fe or Ni. Regarding Pb, Igeo readings range from unpolluted to moderately polluted. **Elnazer *et al.* (2015)** found the same thing for Pb, where the Igeo values for Pb denote that the sediment samples are

uncontaminated to moderately contaminated, and the Igeo results for Cd denote the human input of Cd into soil, with the majority of samples falling into the moderately contaminated class, and just 5 samples being classified as uncontaminated to moderately contaminated with Cd.

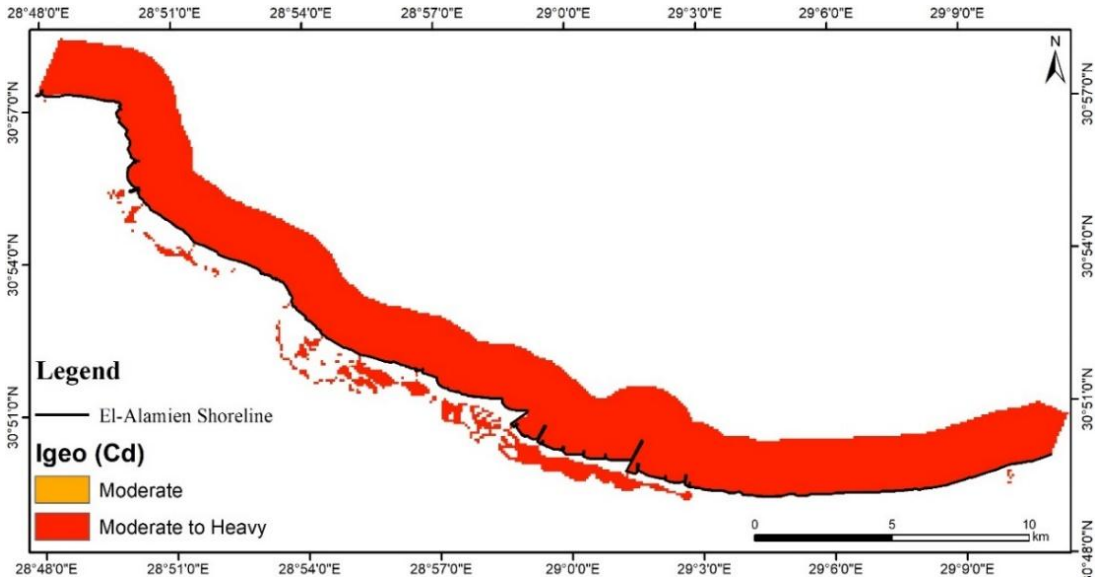

Fig (31): Spatial distribution map for Igeo of Cd in sediment

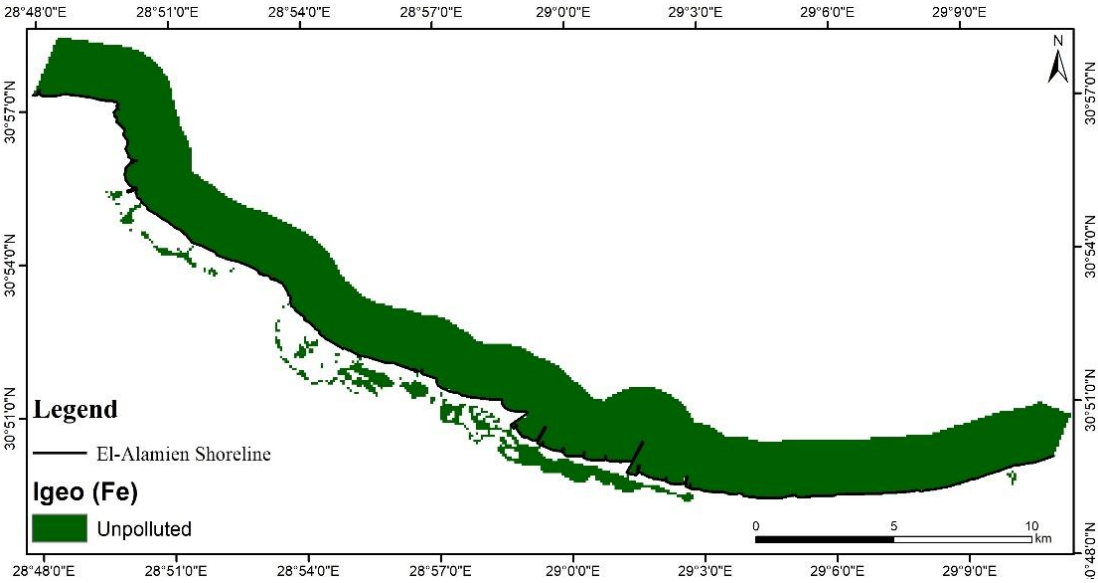

Fig (32): Spatial distribution map for Igeo of Fe in sediment

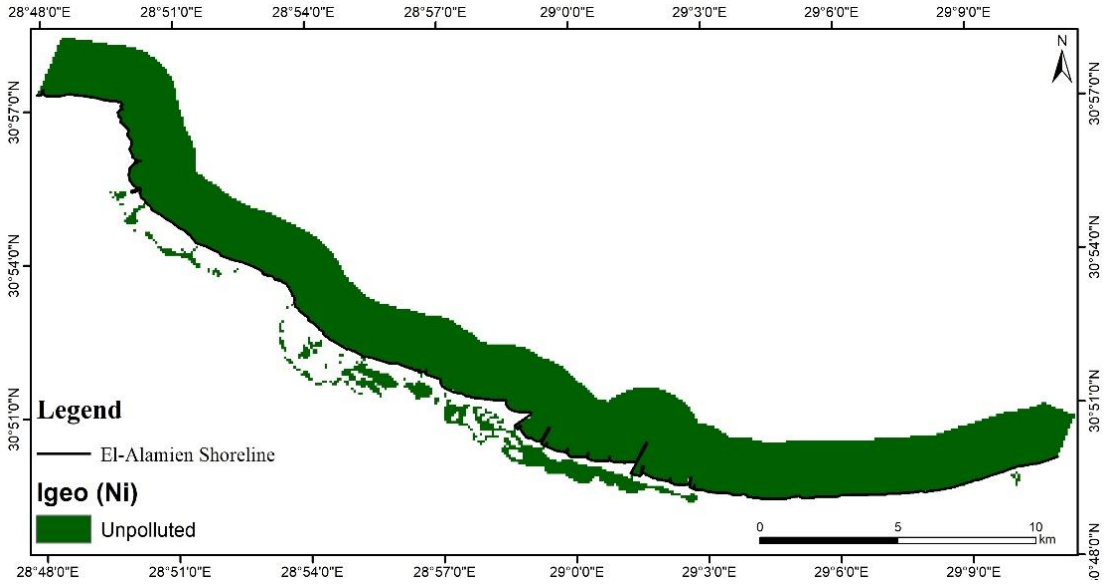

Fig (33): Spatial distribution map for Igeo of Ni in sediment

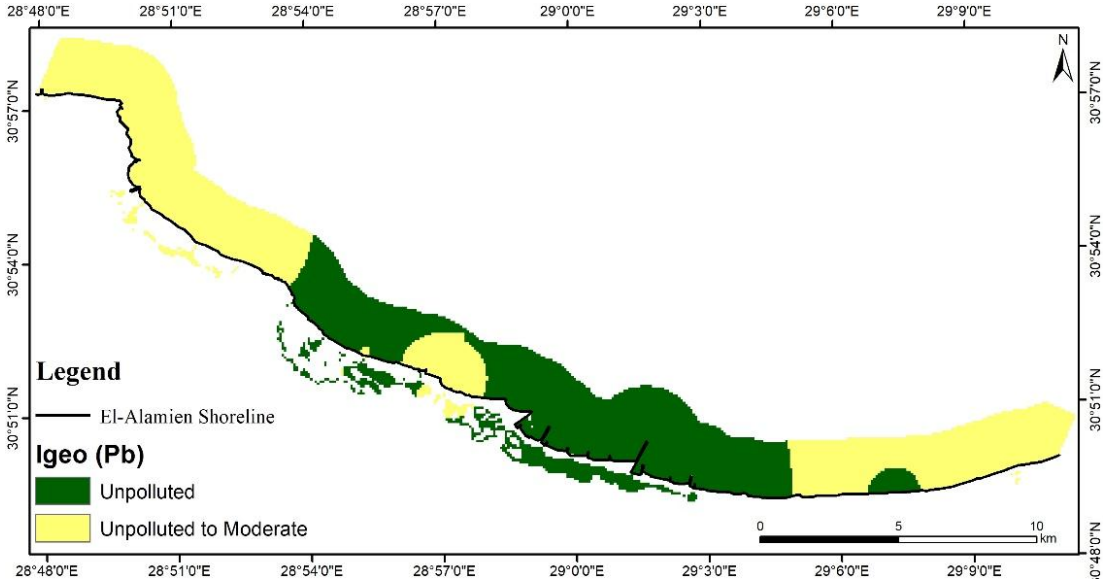

Fig (34): Spatial distribution map for Igeo of Pb in sediment

4. Future coastal changes (DSAS)

Five different dates of El-Alamein shoreline were digitized (1990, 1995, 2000, 2010, and 2020) to be used for the prediction of 2030 shoreline which was obtained by using DSAS tool and the result was shown in Fig. 35. It was obvious that the resulting shoreline is mostly affected by retreat process especially in the middle part of the study region. El-Alamein Shoreline is showing an erosion and an accretion at different rates **(Hammad *et al.*, 2022).**

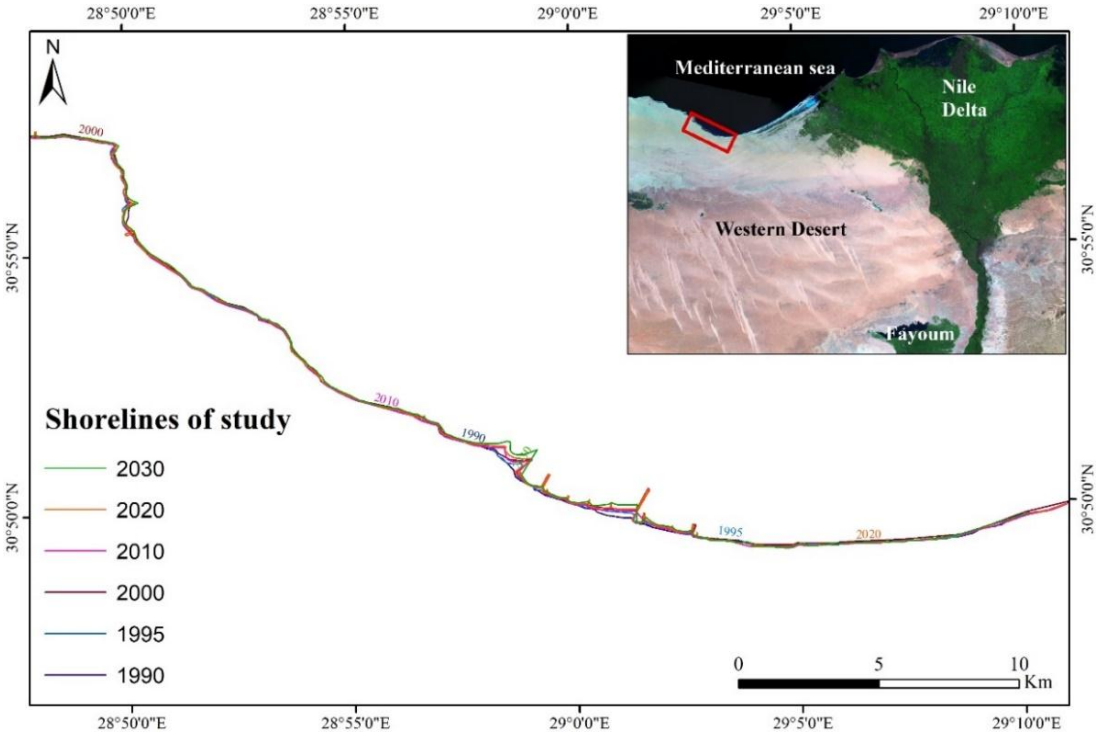

Fig (35): The 6 studied shorelines

The map shown in Fig. 36 presents the retreat of the future shoreline (2030) compared to the shoreline of 2020.

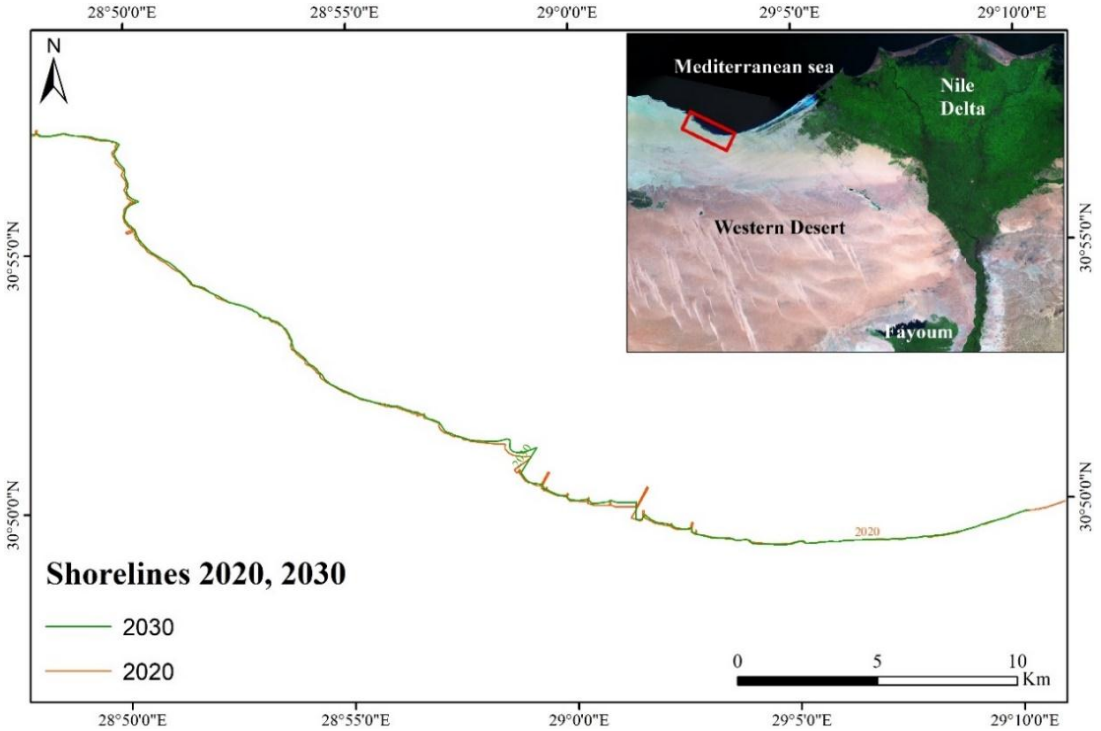

Fig (36): Shorelines of the years 2020 and 2030.

The erosion and accretion in the next decade for the studied area shoreline were predicted and it was obvious that the area will be affected by accretion (1.793 km^2) more than erosion (0.361 km^2) till the year 2030. The annual rate of accretion and erosion will be 0.18 and 0.04 km^2/year, respectively (Fig. 37).

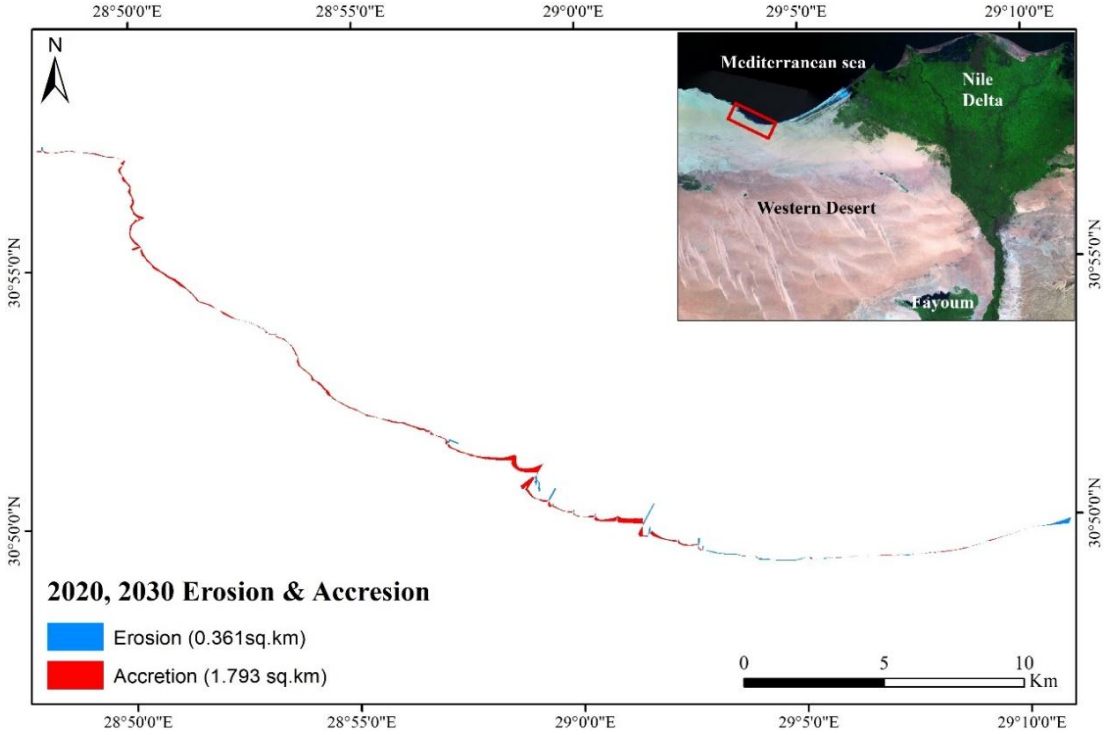

Fig (37): Erosion and accretion from 2020 to 2030.

5. El-Alamein degradation map

A final degradation map was produced to assess the overall deterioration in the area resulting from erosion (actual and predicted) and contamination in the area (Fig. 38). It was obvious that the whole area is moderately contaminated which might be due the anthropogenic activities associated with the new constructions in El-Alamein. Also, the actual erosion dominated the eastern and western parts of the area, and the predicted erosion will dominate in the eastern parts.

The pollution sources and the water flow direction have a significant impact on water quality characteristics. However, persistent sources of pollution have a significant influence on sediment quality features, resulting in the aggregation of contaminants in the bottom sediments **(El-Zeiny *et al*., 2019)**.

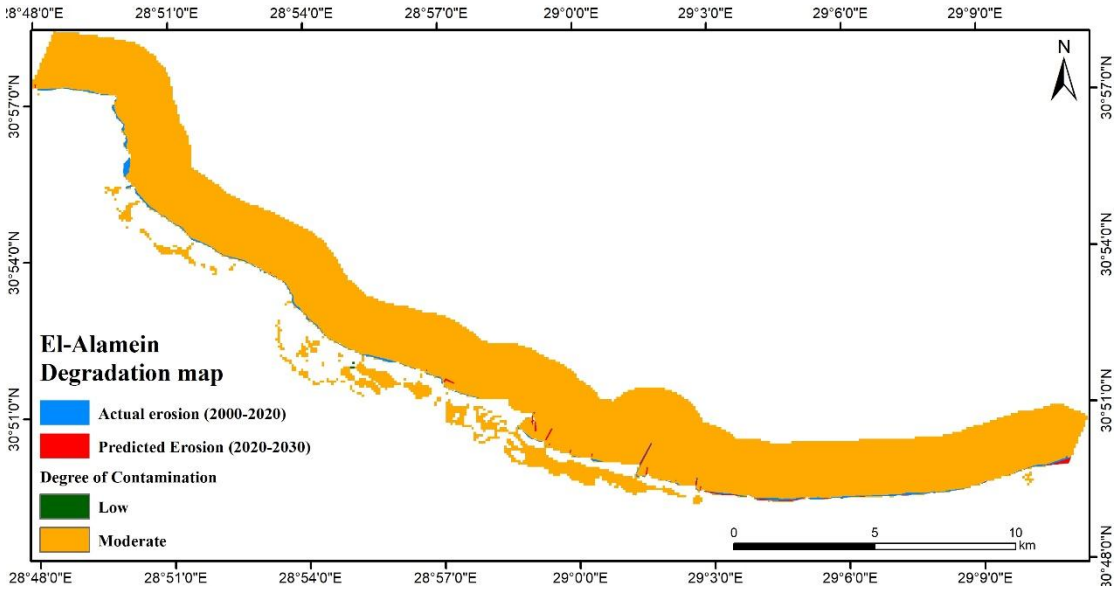

Fig. (38): El-Alamein degradation map.

CONCLUSION

Remote sensing imagery integrated with spatial analyses of water and sediment helped to predict the future shoreline erosion and to assess the environmental quality/ contamination of El-Alamein coastal area. It can be concluded that the research area is affected by a moderate contamination degree because of the high levels of Cd and Pb however, the overall ecological risk is still low. Further, the area will be subjected to more accretion than erosion in the next decade (2020 to 2030) according to the prediction analyses using DSAS. To sustain the marine ecosystem of El-Alamein and prevent the occurrence of any degradation, it's recommended that water and sediment quality/ contamination should be studied regularly and continuously. In addition, shoreline erosion and accretion should be monitored regularly for any unexpected coastal change, to conserve the infrastructure in the region.

ACKNOWLEDGEMENT

Authors acknowledge the Academy of Scientific Research and Technology (ASRT) for financial support provided through the SNG scholarship and the National Authority for Remote Sensing and Space Sciences (NARSS) for continuous support and help.

REFERENCES

- **Abou Samra, R.M. and El-Barbary, S.M.** (2018). The use of remote sensing indices for detecting environmental changes: a case study of North Sinai, Egypt. Spat. Inf. Res., 26: 679–689.

- **APHA,** (1992). Standard Methods for the Examination of Water and Wastewater. Washington, 18th ed. DC. 1.
- **Baig, M.R.I.; Ahmad, I.A.; Shahfahad; Tayyab, M. and Rahman, A.** (2020). Analysis of shoreline changes in Vishakhapatnam coastal tract of Andhra Pradesh, India: an application of digital shoreline analysis system (DSAS), Annals of GIS, 26:4: 361-376, DOI:10.1080/19475683.2020.1815839
- **Bhateria, R. and Jain, D.** (2016). Water quality assessment of lake water: a review.
- **Bresline, V.T. and Sanudo-Wilhelmy, S.A.** (1999). High spatial resolution sampling of metals in the sediment and water column in port Jefferson Harbor, New York. Estuaries., 22: 669–680.
- **Bruland, K.W.; Bertine, K.; Koide, M. and Goldberg, E.D.** (1974). History of metal pollution in southern California coastal zone. Environmental Science and Technology., 8: 425–432. Bull. 11 (2): 67–74.
- **Censi, P.A.O.L.O.; Spoto, S.E.; Saiano, F.I.L.I.P.P.O.; Sprovieri, M.; Mazzola. S.; Nardone, G.; Di Geronimo, S.I.; Punturo, R. and Ottonello, D.** (2006). Heavy metals in coastal water systems. A case study from the northwestern Gulf of Thailand. Chemosphere., 64(7): 1167-1176.
- **Cooke, G.D.; Welch, E.B.; Peterson, S.A. and Newroth, P.R.** (1993). Restoration and Management of Lakes and Reservoirs. Lewis Publishers, Boca Raton.
- **Deely, J.M. and Fergusson, J.E.** (1994). Heavy metal and organic matter concentration and distributions in dated sediments of a small estuary adjacent to a small urban area. The Science of the Total Environment., 153: 97–111.
- **Dickinson, W.W.; Dunbar, G.B. and McLeod, H.** (1996). Heavy metal history from cores in Wellington Harbor, New Zealand. Environmental Geology., 27: 59–69.
- **Din, T.B.** (1992). Use of aluminum to normalize heavy metal data from estuarine and coastal sediments of straits of Melaka. Marine Pollution Bulletin., 24: 484–491.
- **El-Banna, M.M. and Hereher, M.E.** (2009). Detecting temporal shoreline changes and erosion/accretion rates, using remote sensing, and their associated sediment characteristics along the coast of North Sinai, Egypt. Environmental Geology., 58: 1419–1427.
- **El-Kammar, A.** (1974). Comparative mineralogical and geochemical study on some Egyptian phosphorites from Nile Valley, Qusier area and Kharga Oasis, Egypt [Ph.D. thesis], Cairo University.

- **El-Matary, F.** (2006). Studies of some Environmental Hazards along the Nile Delta Coastal area between Damietta and Port Said – Egypt. M.Sc. thesis. Damietta, Fac. Of Science. Mans. Univ.
- **Elnazer, A.A. and Salman, S.A.** (2021). Critical load model and pollution indices application for water–soil–plant system assessment around El‑ Hammam canal, East El‑ Alamein, Egypt. International Journal of Environmental Science and Technology
- **Elnazer, A.A.; Salman, S.A.; Seleem, E.M. and Abu El Ella, E.M.** (2015). Assessment of some heavy metals' pollution and bioavailability in roadside soil of Alexandria-Marsa Matruh Highway, Egypt. International Journal of Ecology.
- **El-Rayis, O.A.; Thabet, W.M.; Hussein, R.A. and Hemeda, I.E.** (2012). Assessment of water quality in Alamein Marina Recreational Lagoon. The Journal of The Egyptian Public Health Association., 87(5 and 6): 116-123.
- **El-Zeiny, A.; El Kafrawy, S. and Ahmed, M.** (2019). Geomatics based approach for assessing Qaroun Lake pollution. The Egyptian Journal of Remote Sensing and Space Sciences., 22 (2019): 279–296.
- **Emam, W.W.M. and Soliman, K.M.** (2020). Applying geospatial technology in quantifying spatiotemporal shoreline dynamics along Marina El-Alamein Resort, Egypt. Environ. Monit. Assess., pp.192: 459.
- **EPA (Environmental Protection Agency),** (2017). National Recommended Water Quality Criteria- Aquatic Life Criteria; Appendix A.
- **Genz, A.S.; Fletcher, C.H.; Dunn, R.A.; Frazer, L.N. and Rooney, J.J.** (2007). The predictive accuracy of shoreline change rate methods and alongshore beach variation on Maui, Hawaii. Journal of Coastal Research, 231:87–105. Doi:10.2112/05-0521.1.
- **Gratani, L.; Taglioni, S. and Crescente, M.F.,** (1992). "The accumulation of lead in agricultural soil and vegetation along a highway," Chemosphere, 24(7): 941–949.
- **Hakanson, L.** (1980). An ecological risk index for aquatic pollution control. A sedimentological approach. Water Res., 14 (8): 975–1001.
- **Hammad, H.; El-Zeiny, A.; Abu El-Hassan, M. and Khalifa, M.** (2022). Remote sensing and GIS for monitoring coastal changes in El-Alamein area, Matrouh, Egypt. Journal of Environmental and Energy Research, 11 (9).
- **Hornung, H.; Karm, M.D. and Cohen, Y.** (1989). Trace metal distribution on sediments and benthic fauna of Haifa Bay, Israel. Estuarine, Coastal and Shelf Science., 29: 43–56.
- **Jones, R.A. and Lee, G.F.** (1986). Eutrophication modeling for water quality management: an update of the Vollenweider-OECD model. World Health Org. Water Qual.

- **Matthai, C. and Birch, G.** (2001). Detection of anthropogenic Cu, Pb, and Zn in continental shelf sediments off Sydney, Australia – A new approach using normalisation with cobalt. Marine Pollution Bulletin., 42: 1055–1063.
- **Mortatti, J. and Probst, J.** (2010). Characteristics of heavy metals and their evaluation in suspended sediments from Piracicaba River basin (S~ao Paulo, Brazil). Revista Brasileira de Geociˆencias., 40: 375–379.
- **Müller, G.** (1969). Index of geo-accumulation in the sediments of the Rhine River. Geo-journal., 2: 108–118.
- **Murali, R.M.; Ankita, M.; Amrita, S. and Vethamony, P.** (2013). "Coastal vulnerability assessment of Puducherry coast, India, using the analytical hierarchical process." Natural Hazards and Earth System Sciences., 13 (12): 3291–3311. doi:10.5194/ nhess-13-3291-2013.
- **Nan, Z.R.; Wenqung, X. and Zhao, C.Y.** (2006). "Spatial distribution of selected trace metals in urban soils of Lan-Zhou city, Gansu province, Northwestern of China," in Proceedings of the IEEE International Geoscience and Remote Sensing Symposium (IGARSS '06)., pp. 3397–3400, Denver, Colo, USA, August 2006.
- **Nassar, K.; Mahmod, W.E.; Fath, H.; Masria, A.; Nadaoka, K.; and Negm, A.** (2019). Shoreline change detection using DSAS technique: Case of North Sinai coast, Egypt. Marine Geo-resources & Geotechnology., 37(1): 81-95.
- **Niencheski, L.F.; Windom, H.L. and Smith, R.** (1994). Distribution of particulate trace metal in Patos Lagoon Estuary (Brazil). Marine Pollution Bulletin., 28: 96–102.
- **Okorie, I.A.** (2010). Determination of potentially toxic elements (PTEs) and an assessment of environmental health risk from environmental matrices [Ph.D. thesis], School of Applied Sciences Northumbria University.
- **Ravichandran, M.; Baskaran, M.; Santschi, P.H. and Bianchi, T.** (1995). History of trace metal pollution in Sabine-Neches Estuary, Beaumont, Texas. Environmental Science and Technology., 29: 1495–1503.
- **Salomons, W. and Förstner, U.** (1984). Metals in the hydro-cycle. Springer, Berlin Heidelberg Tokyo.
- **Semerjian, L.** (2010). "Equilibrium and kinetics of cadmium adsorption from aqueous solutions using untreated Pinus halepensis sawdust," Journal of Hazardous Materials, vol. 173, no. 1–3, pp. 236– 242, 2010.
- **Sharma, V.K.; Rhudy, K.B.; Koenig, R.; Baggett, A.T.; Hollyfield, S. and Vazquez, F.G.** (1999). Metals in sediments of Texas estuaries, USA. Journal of Environmental Science and Health, 34, 2061–2073.
- **State Information Service** (2018). Al-Alamein: From war and destruction to development and construction. [pdf] Cairo: Information sector, Central Department of editing, translations, and bulletins.

- **Stewart, C.** (1989). Spatial and temporal trends in trace metal deposition in Canterbury, New Zealand. Ph.D. thesis, University of Canterbury, Christchurch, New Zealand.
- **Stoffers, P.; Glasby, G.P.; Wilson, C.J.; Davis, K.R. and Watter, P.** (1986). Heavy metal pollution in Wellington Harbor. New Zealand Journal of Marine and Freshwater Research, 20, 495–512. Sustain. Water Resour. Manage., 2: 161–173.
- **Thieler, E.R.; Himmelstoss, E.A.; Zichichi, J.L. and Ergul, A.** (2009). Digital Shoreline Analysis System (DSAS) version 4.0—an ArcGIS extension for calculating shoreline change. Open-File Report. U.S. Geological Survey Report No. 2008– 1278.
- **Tomlinson, D.L.; Wilson, J.G.; Harris, C.R. and Jeffrey, D.W.** (1980). Problems in the assessment of heavy-metal levels in estuaries and the formation of a pollution index. Helgoländer meeresunter suchungen., 33 (1): 566.
- **Turekian, K.K. and Wedepohl, K.H.** (1961). Distribution of the elements in some major units of the earth's crust. Geol. Soc. Am. Bull., 72 (2): 175–192.
- **Windom, H.L.; Smith, J.r.; R.G. and Rawlinson, C.** (1989). Particulate trace metal composition and flux across the southeastern US continental shelf. Marine Chemistry., 27: 283–297.
- **Zeng, X. and Rasmussen, T.C.** (2005). Multivariate statistical characterization of water quality in Lake Lanier, Georgia, USA. J. Environ. Qual., 34 (6): 1980–1991.
- **Zheng, X.; Zang, W.; Yan, Z.; Hong, Y.; Liu, Z.; Yi, X.; Wang, X.; Liu, T.; and Zhou, L.** (2015). Species sensitivity analysis of heavy metals to freshwater organisms. Ecotoxicology., 24:1621–1631.